The Solar Corona
and Inner Heliosphere

Jaroslav Dudík [1,2]

[1] – DAPEM, Faculty of Mathematics, Physics and Informatics,
Comenius University, Bratislava, Slovakia
[2] – Astronomical Institute of the Academy of Sciences
Ondřejov, Czech Republic

ISWI-Europe Summer School in Space Science,
AISAS, Tatranská Lomnica, August 22, 2011

Outline

I. **The Solar Corona and Wind: Basic Properties**
   White-light corona from eclipses
   Solar wind

II. **Observations: Towards Imaging Spectroscopy**
   Basics of spectroscopy of optically thin plasmas
   Instrumentation
   Active regions, Quiet Sun, Coronal holes
   Warm loops, hot loops
   Isothermal vs. DEM, resolved vs. unresolved

III. **The Coronal Heating Problem**
   Scaling laws
   Steady vs. Impulsive
   Forward models of the active region coronae

Solar corona – basic properties

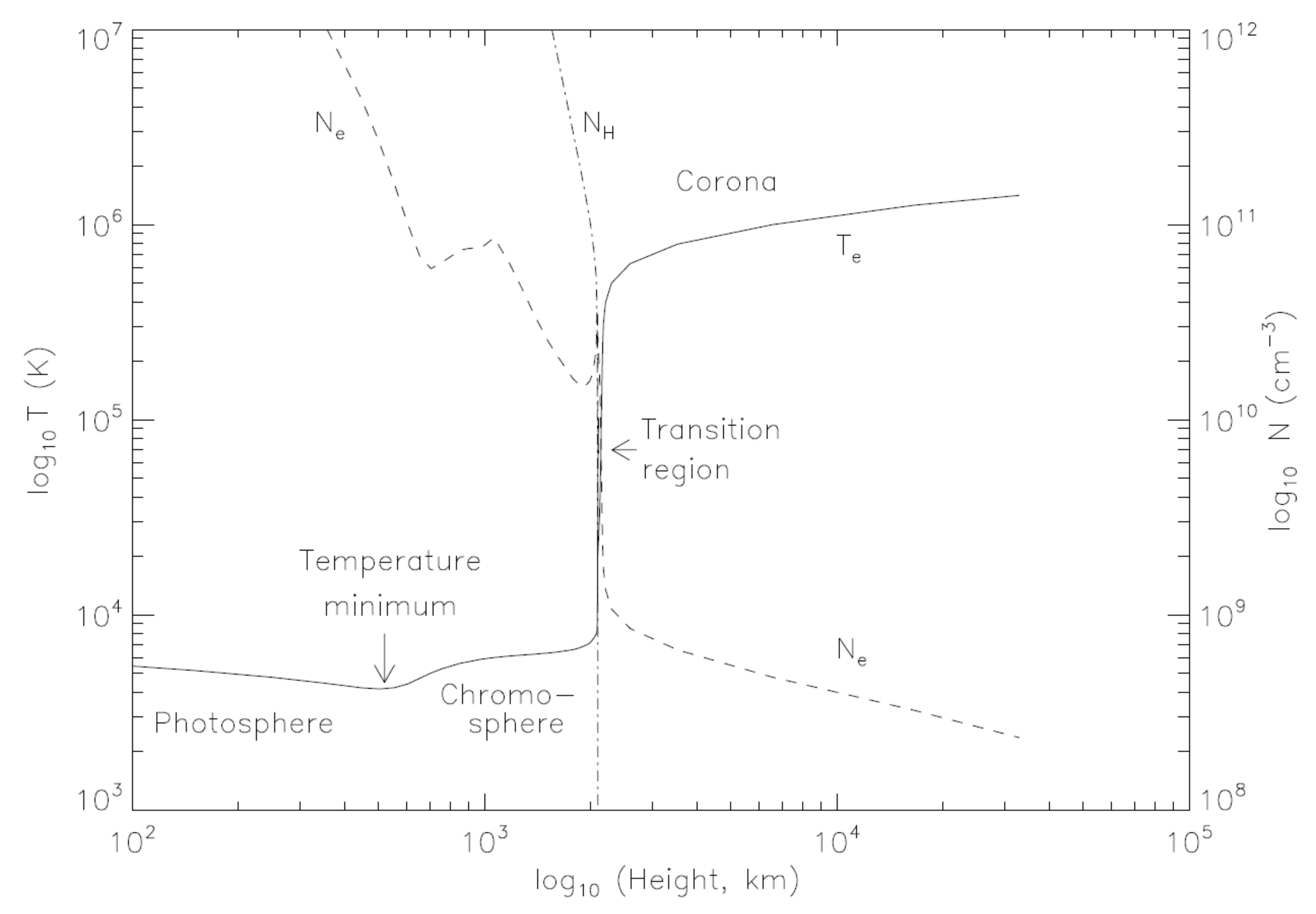

Phillips, Feldman & Landi (2008): UV and X-ray Spectroscopy of the Solar Atmosphere, image after *Gabriel (1976), Vernazza et al. (1981)* and *Fontenla et al. (1990)*

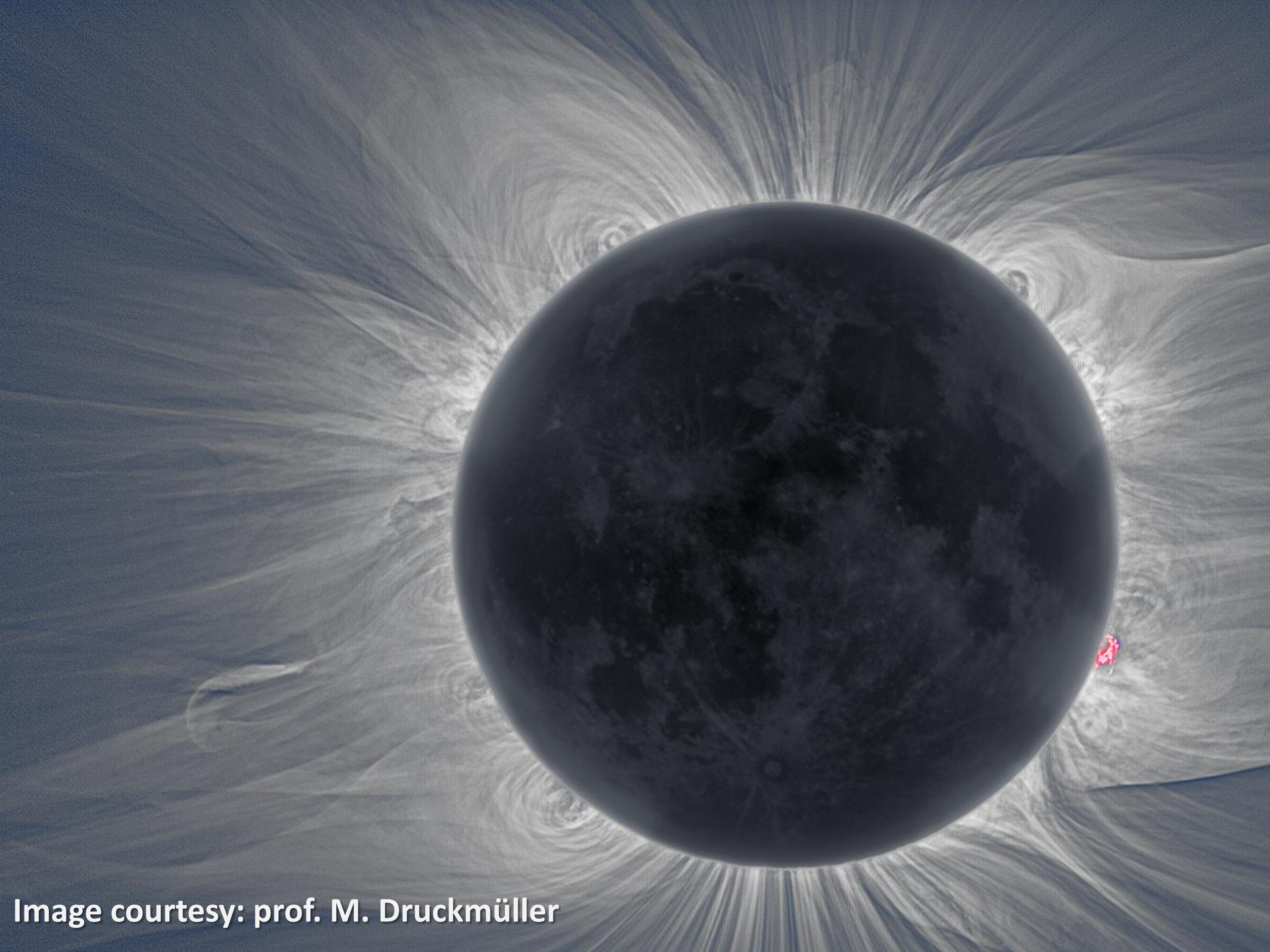
Image courtesy: prof. M. Druckmüller

Image courtesy: prof. M. Druckmüller

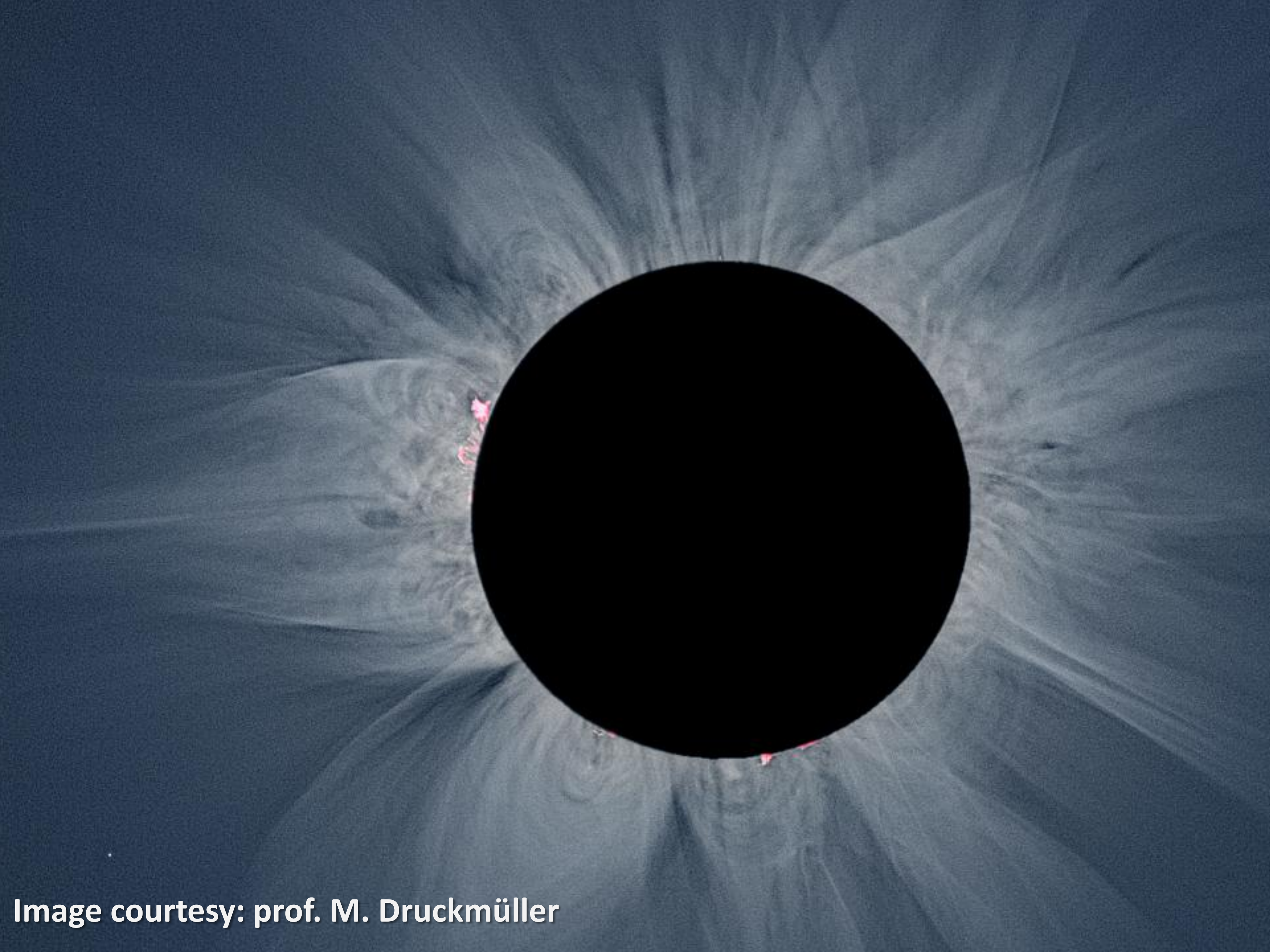

Image courtesy: prof. M. Druckmüller

C/1996 B2 (Hyakutake), image: E. Kolmhofer, H. Raab
Johannes-Kepler-Observatory, Linz, Austria

Solar wind – basic properties

- **Continuous outward stream of particles from the Sun**
  - Consequence: heliosphere
  - 1916, Birkeland: solar wind consists of both positive and negative particles
  - 1958, Parker: Theory of solar wind – supersonic flow
  - 1959, Luna 1: first direct observation of Solar wind

- **Mass loss rate:** $\sim 2 \times 10^{-14}\ M_\odot\ yr^{-1}$

Average	Slow wind	Fast wind	
$n = 8.7 \pm 6.6$	11.9 ± 4.5	3.9 ± 0.6	cm^{-3}
$v = 468 \pm 116$	327 ± 15	702 ± 32	$km.s^{-1}$
$T_e = 1.4 \pm 0.4 \times 10^5$	$1.3 \pm 0.3 \times 10^5$	$1.0 \pm 0.1 \times 10^5$	K
$T_p = 1.2 \pm 0.9 \times 10^5$	$3.4 \pm 1.5 \times 10^4$	$2.3 \pm 0.3 \times 10^5$	K

Solar wind – properties

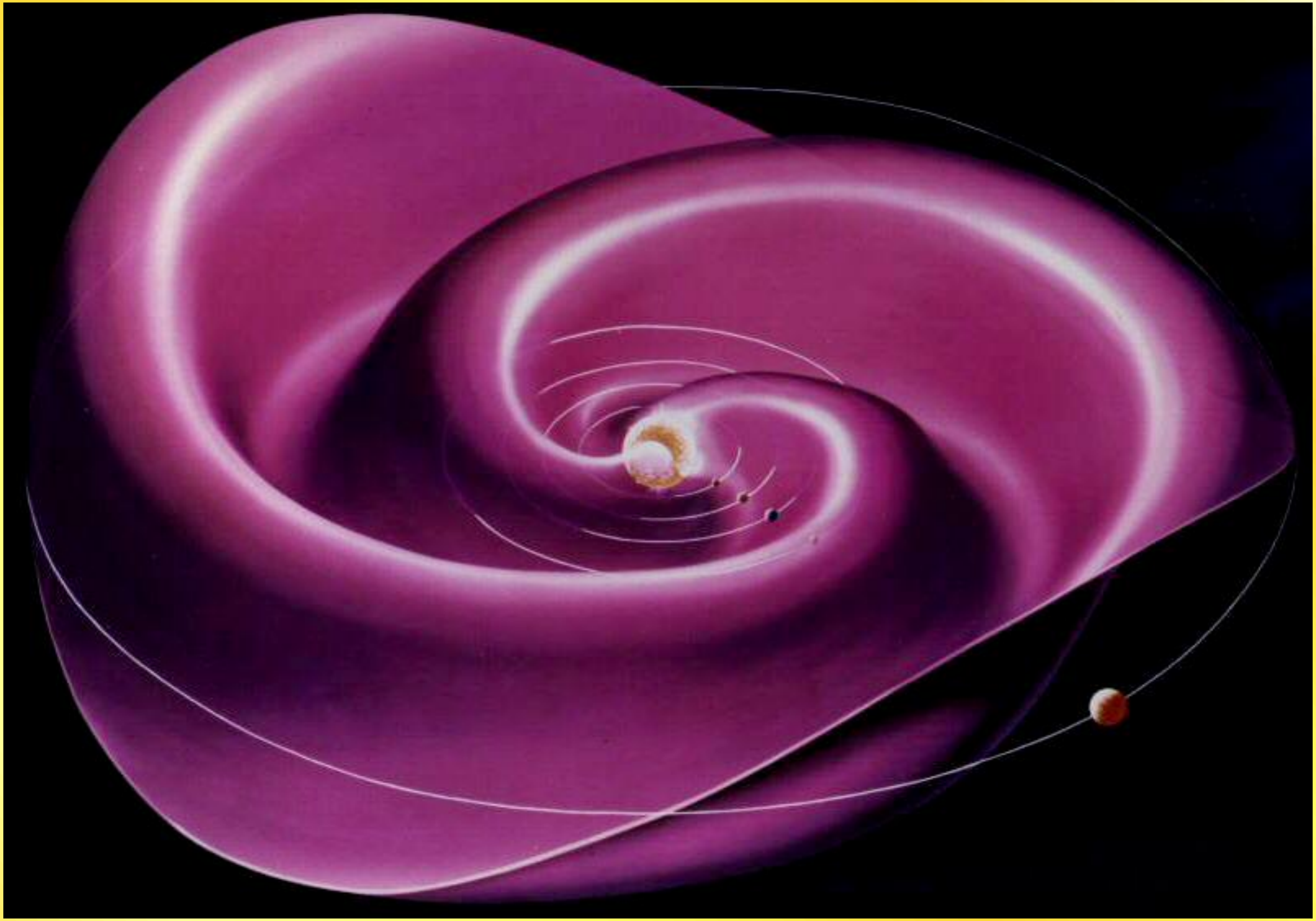

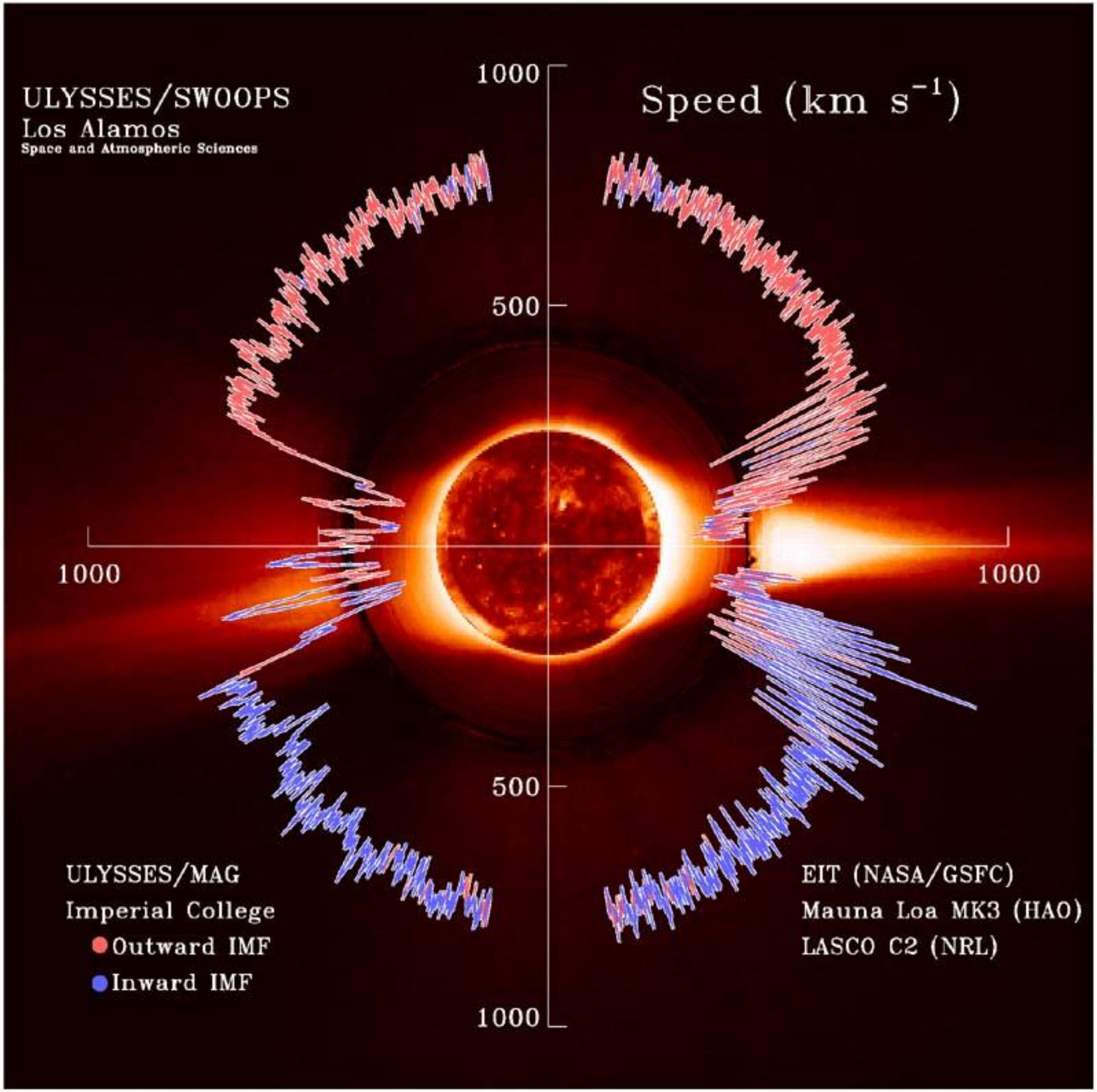
ULYSSES/SWOOPS
Los Alamos
Space and Atmospheric Sciences
Speed (km s^{-1})
1000
500
1000
1000
500
1000
ULYSSES/MAG
Imperial College
Outward IMF
Inward IMF
EIT (NASA/GSFC)
Mauna Loa MK3 (HAO)
LASCO C2 (NRL)

Solar wind – properties

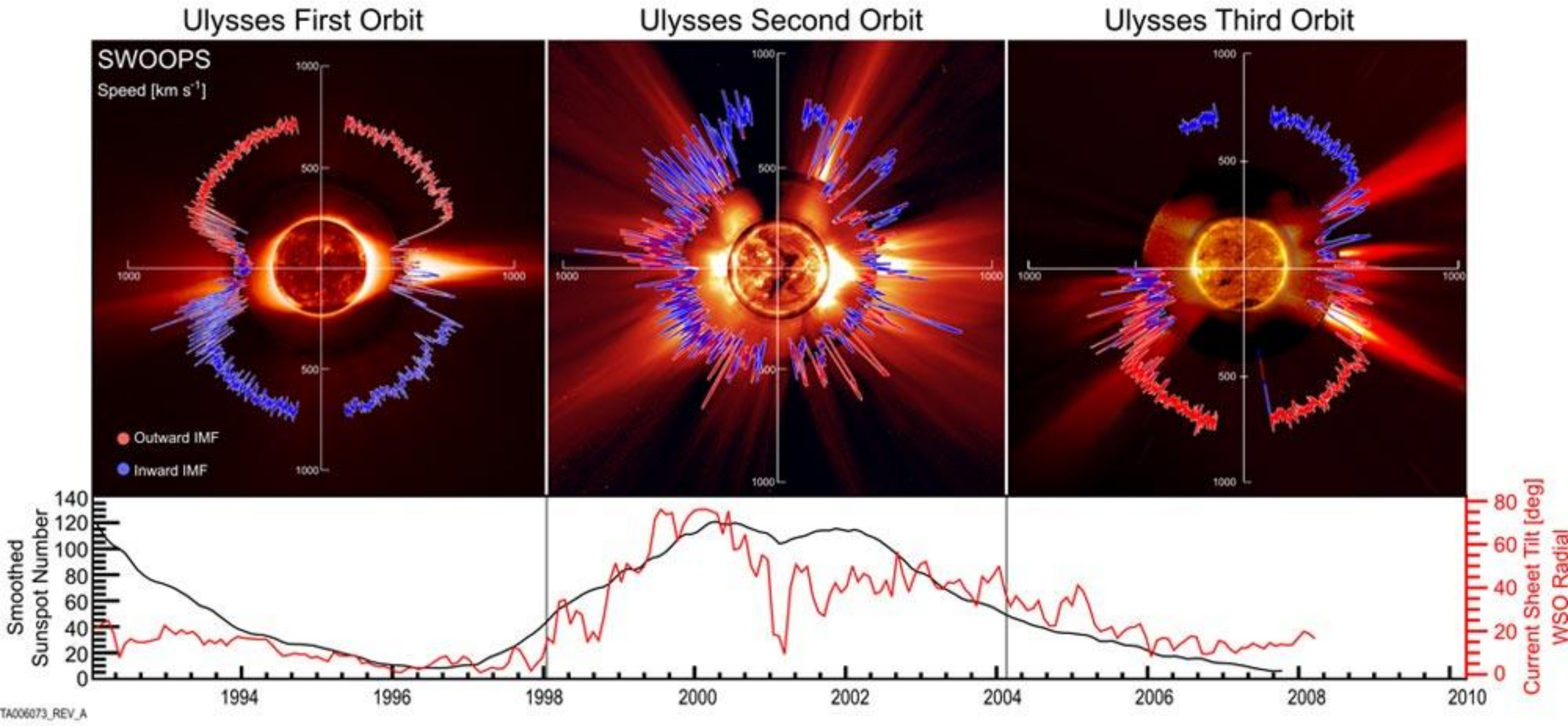

McComas et al. (2008), Geophys. Res. Lett. 35, L18103

Velocity distribution

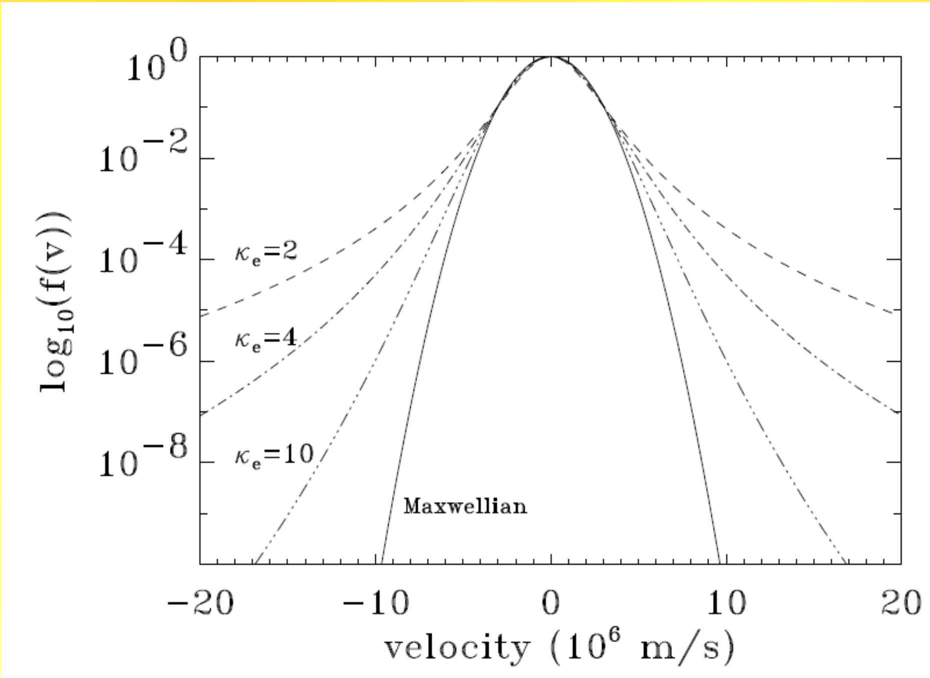

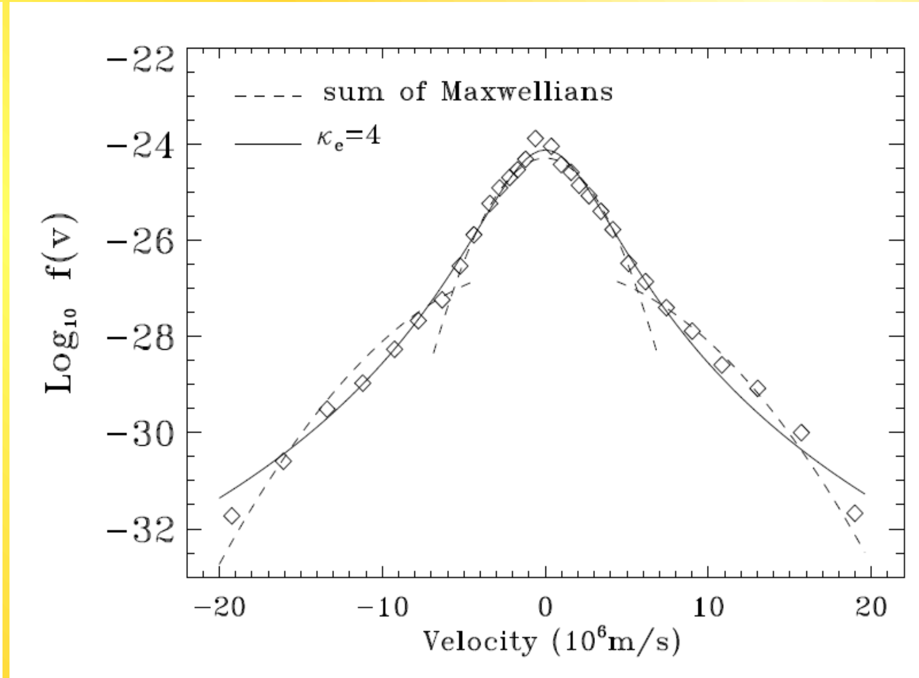

Observed velocity distribution shows non-thermal tails:
The velocity distribution is better fitted by one *κ*-distribution than by one Maxwellian or sum of two Maxwellian distributions

Maksimovic et al. (1997), Astron. Astrophys. 324, 725

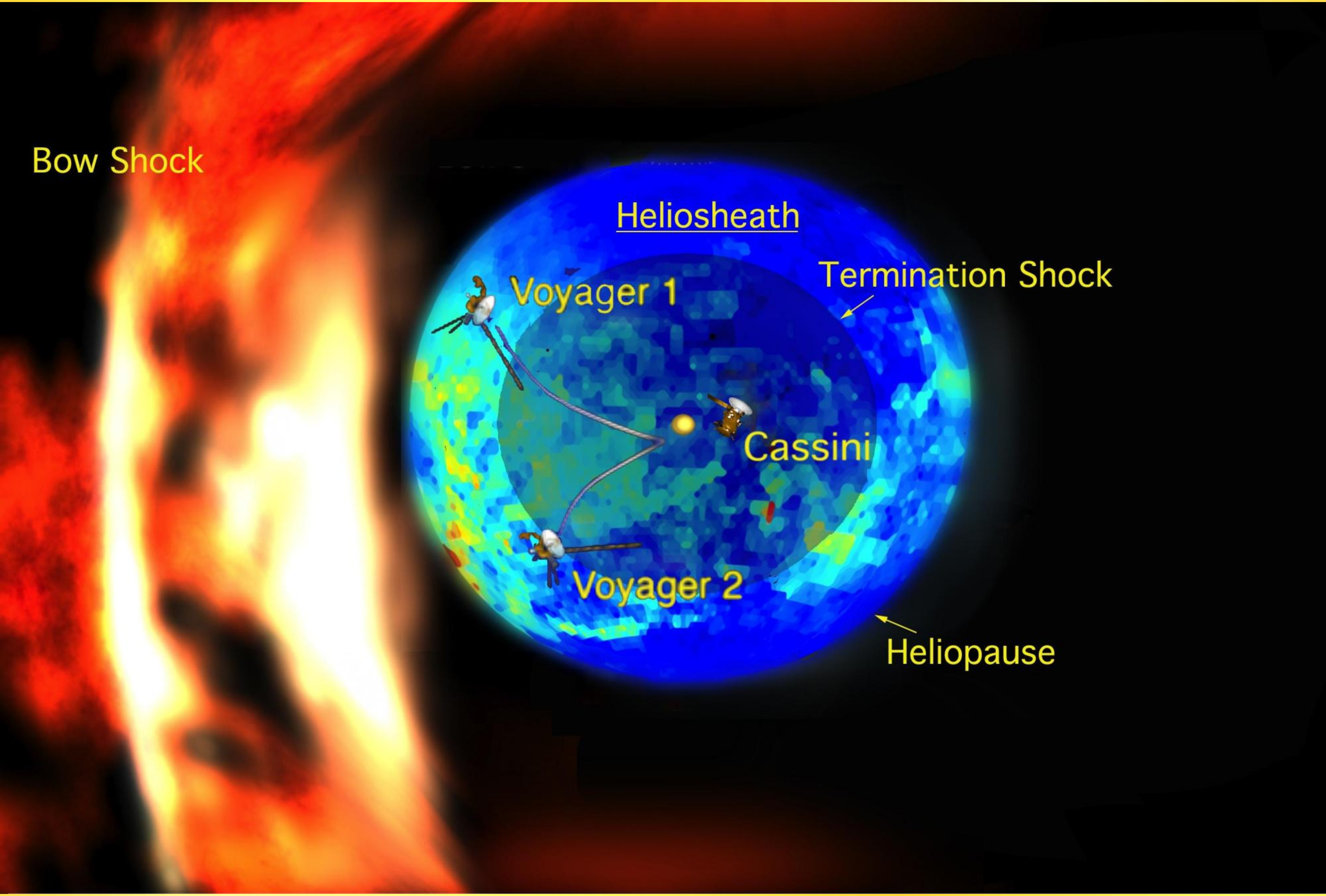

Image credit: NASA/JPL/JHUAPL

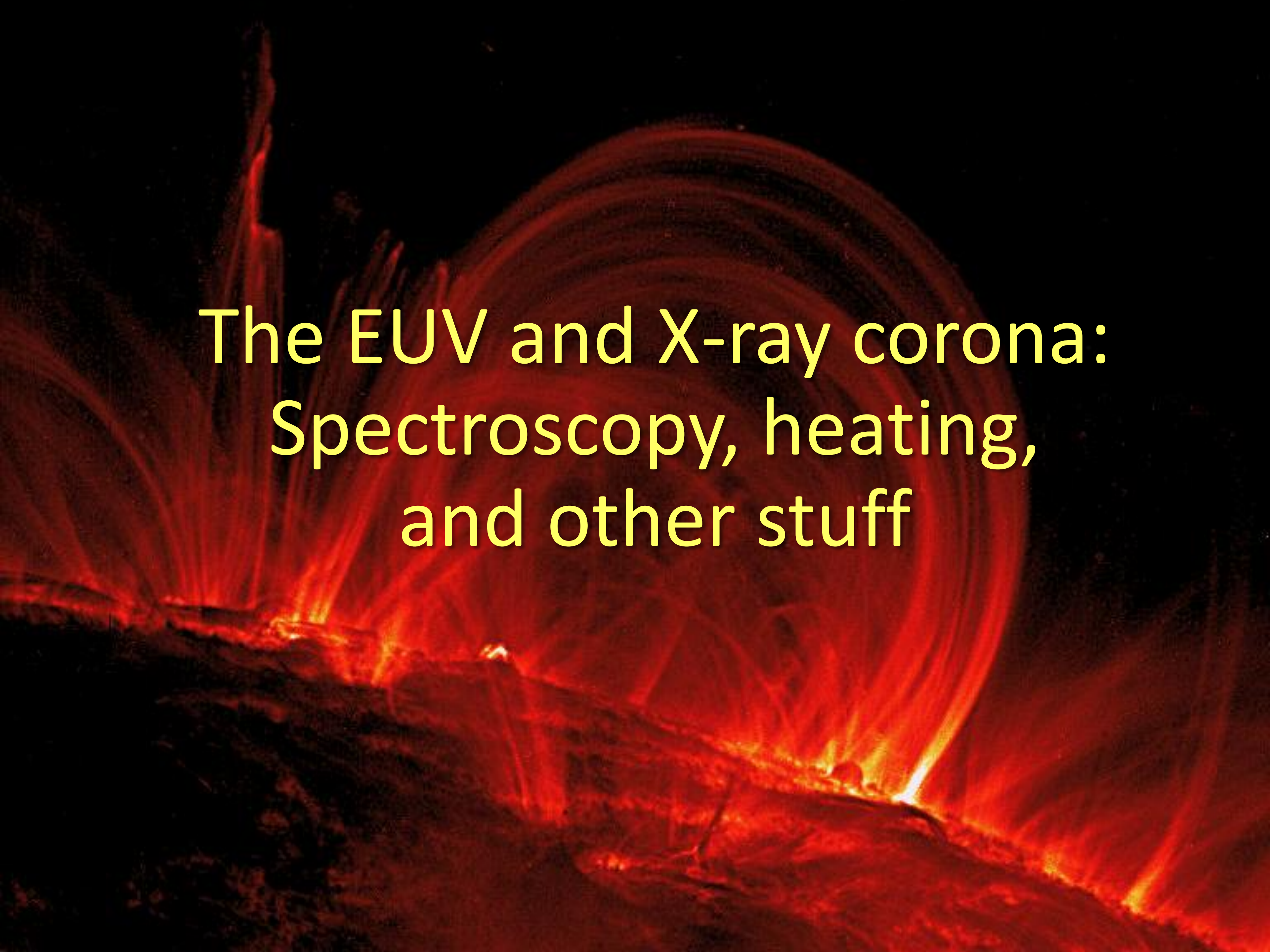

The EUV and X-ray corona: Spectroscopy, heating, and other stuff

Spectroscopy – an introduction

The emissivity ε_{ij} of a spectral line λ_{ij} produced by transitions from level *i* to level *j* in a *k*-times ionized atom of element *x* is given by

$$\varepsilon_{ij} = \frac{hc}{\lambda_{ij}} A_{ij} n_i = \frac{hc}{\lambda_{ij}} \frac{A_{ij}}{n_e} \frac{n_i}{n_k} \frac{n_k}{n_x} \frac{n_x}{n_H} n_H n_e$$

$$= A_x G(T, n_e) n_H n_e$$

Intensity I_{ij} of this emission line arising in optically thin plasmas with volume V is

$$I_{ij} = A_x \int G(T, n_e) n_H n_e dV$$

FIP effect, or the "coronal abundances"

Elements with first ionization potential smaller than 10 keV have greatly enhanced abundances in the corona: FIP effect

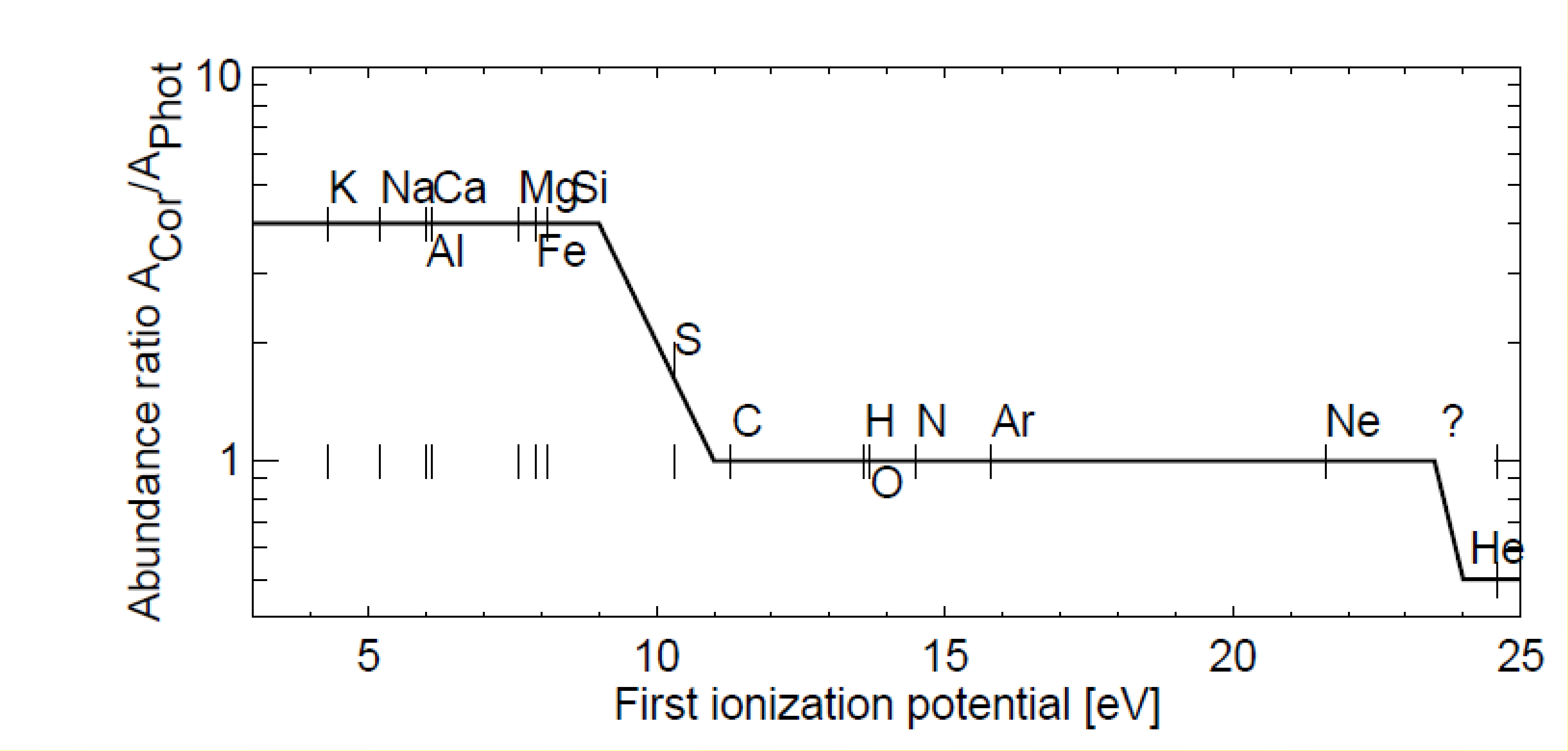

Feldman & Widing (2003), Space Sci. Rev. 107, 665

Ionization equilibrium – Fe

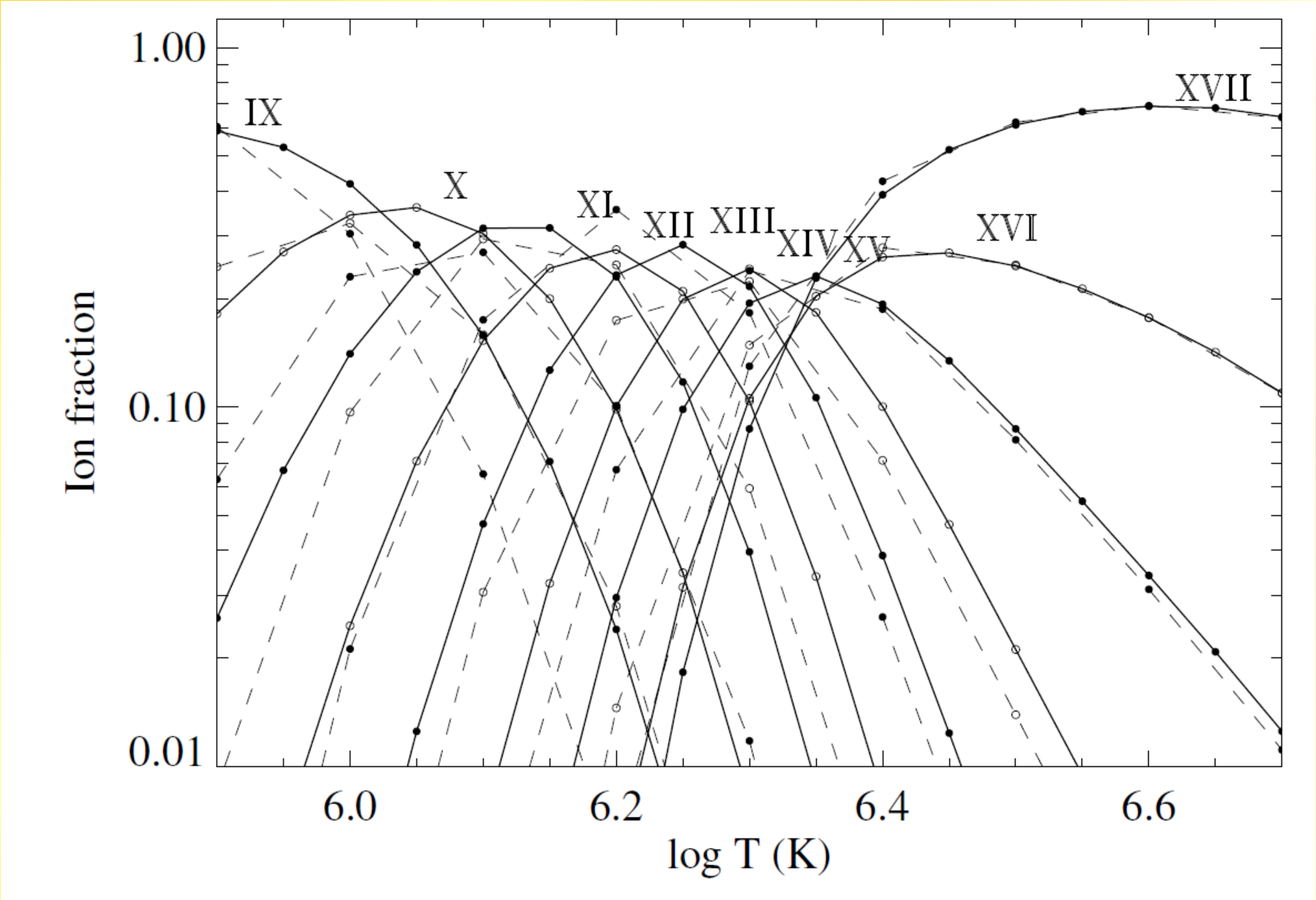

Dere et al. (2009), Astron. Astrophys. 498 915, CHIANTI 6 paper

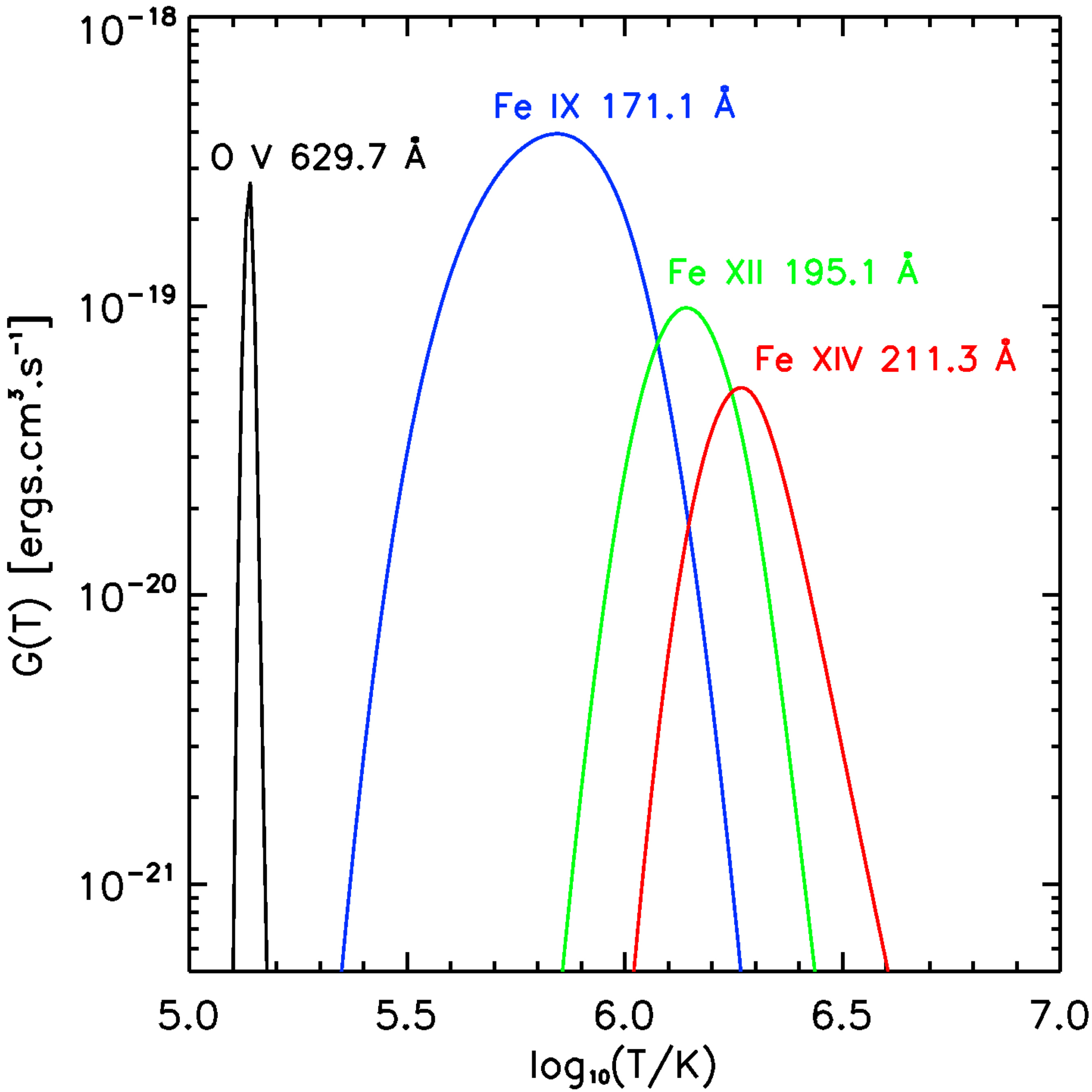

O V 629.7 Å
Fe IX 171.1 Å
Fe XII 195.1 Å
Fe XIV 211.3 Å
10^−18
10^−19
10^−20
10^−21
5.0
5.5
6.0
6.5
7.0
log10(T/K)
G(T) [ergs.cm3.s-1]

EM and DEM(T)

If the plasma is isothermal, the intensity is simply

$$I_{ij} = A_x G(T, n_e) \int n_H n_e dV = A_x G(T, n_e) EM(T).$$

However, if the plasma is multithermal, i.e., has a range of temperatures, the intensity is given by

$$I_{ij} = A_x \int G(T, n_e) n_H n_e \frac{dV}{dT} dT = A_x \int_T G(T, n_e) DEM(T) dT$$

where DEM(T) is the differential emission measure.

EM-loci method

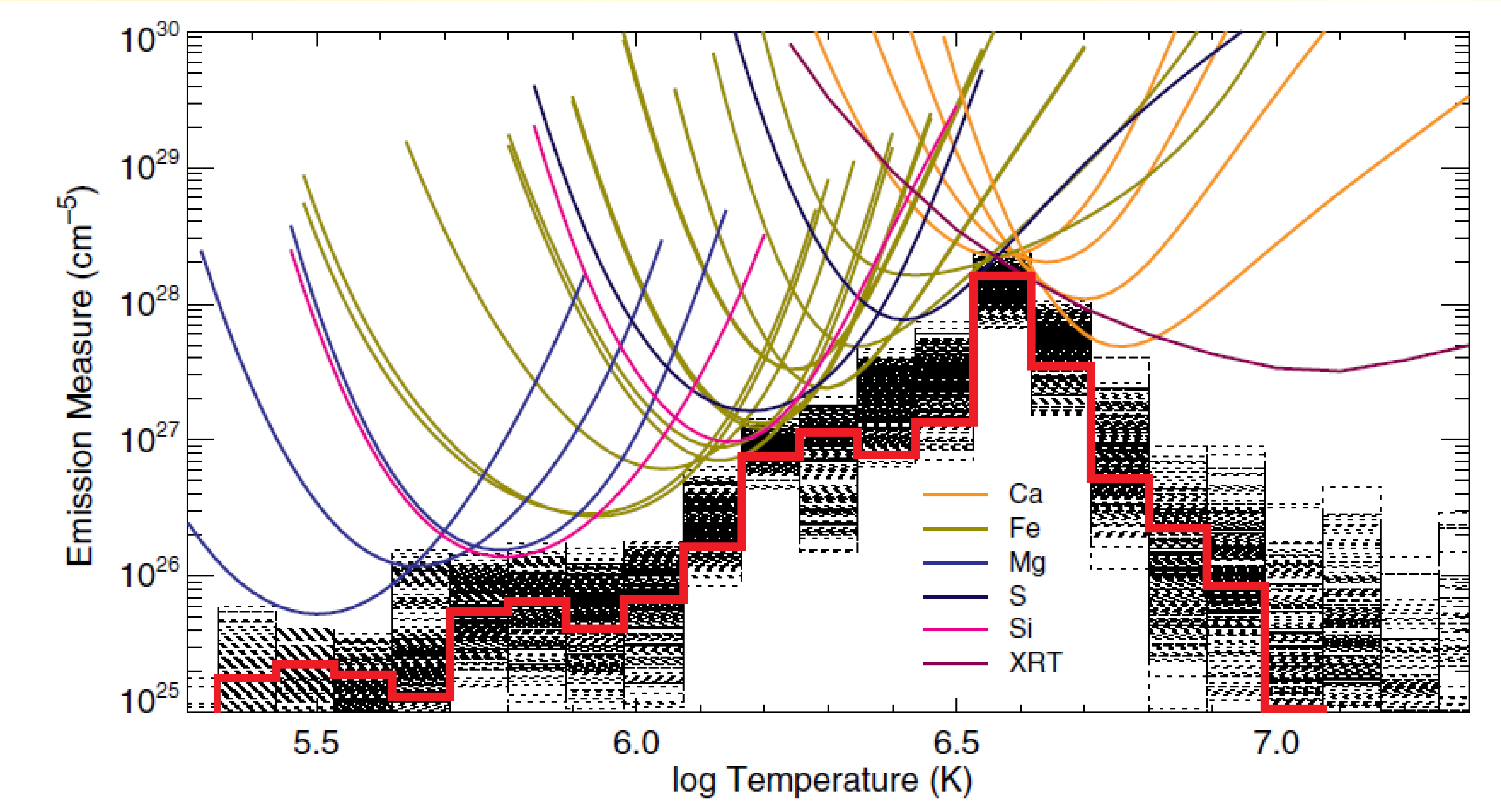

Warren et al. (2011), Astrophys. J. 734, 90

Radiative losses from the corona

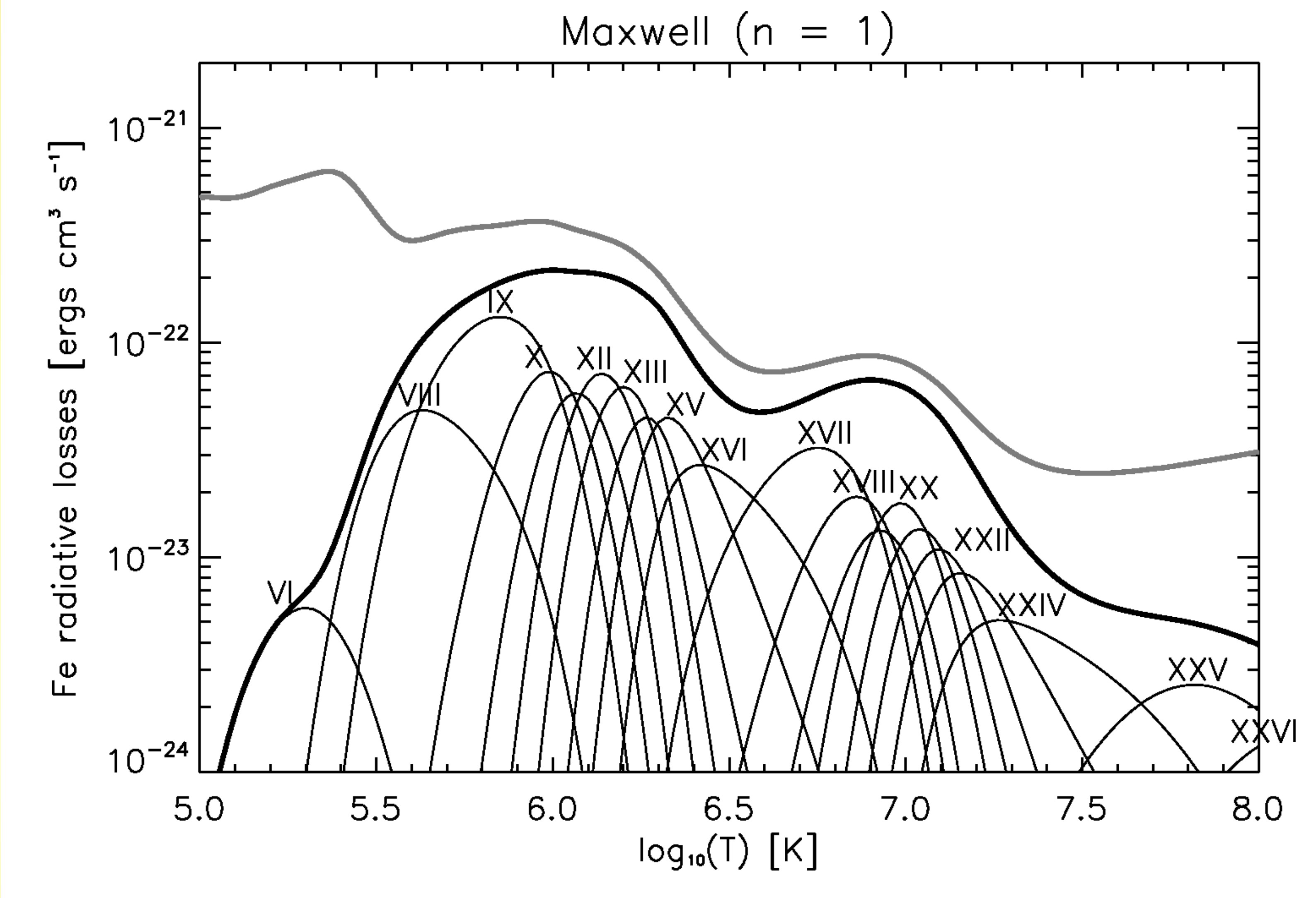

Dudík et al. (2011), Astron. Astrophys. 529, A103

EUV and X-ray filters

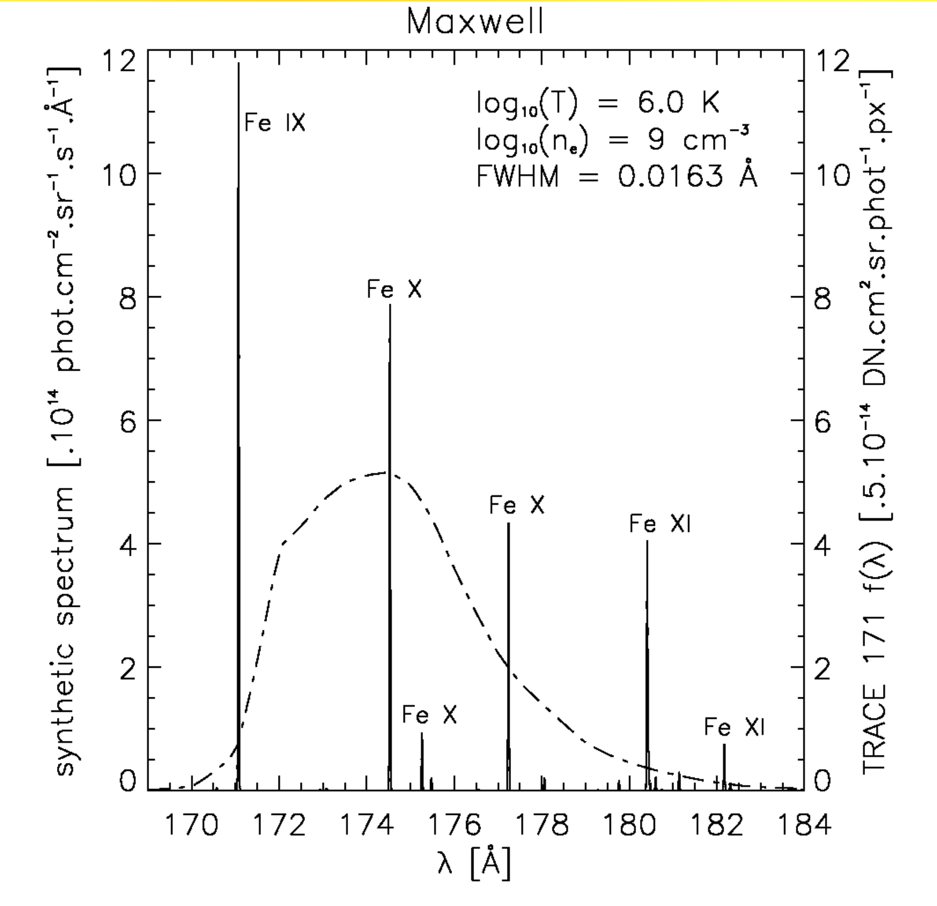

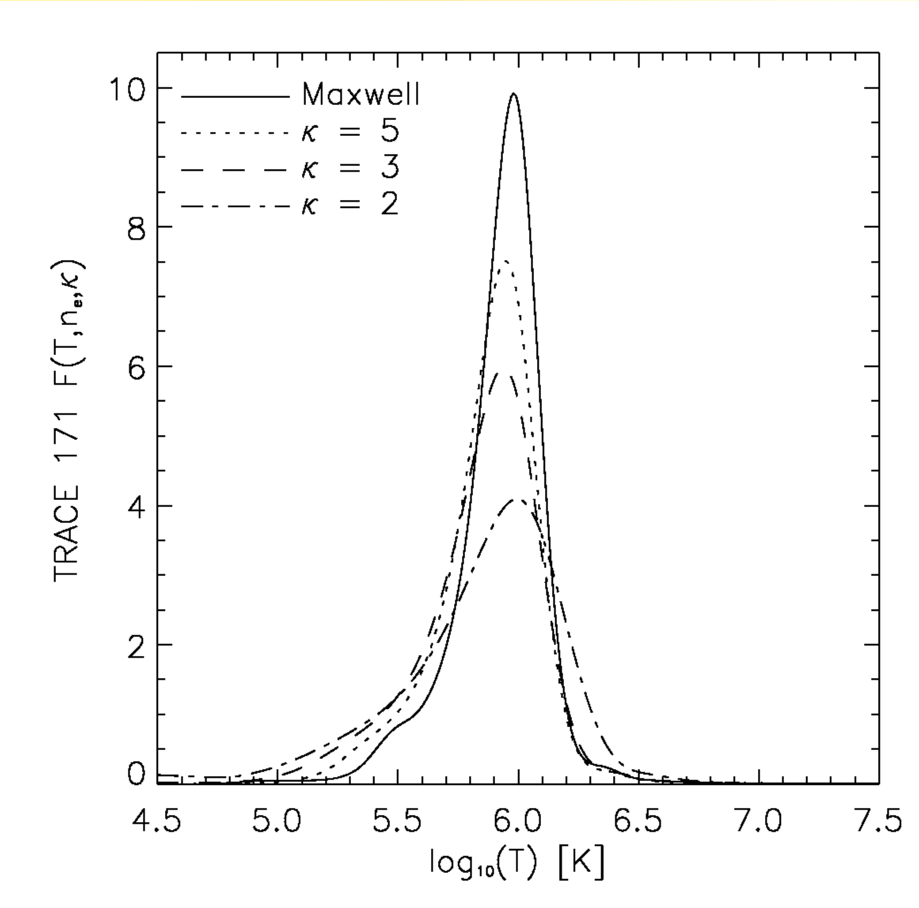

Dudík et al. (2009), Astron. Astrophys. 505, 1255

Hinode/XRT, Hinode/EIS

Hinode (“Sunrise” in japanese)	– Jap. mission, launched 2006
The X-Ray Telescope (**XRT**)	– multi-filter telescope
EUV Imaging Spectrometer (**EIS**)	– 170-210 Å and 250-290 Å
	– slit-slot mech. 1”, 2”, 40”, 266”

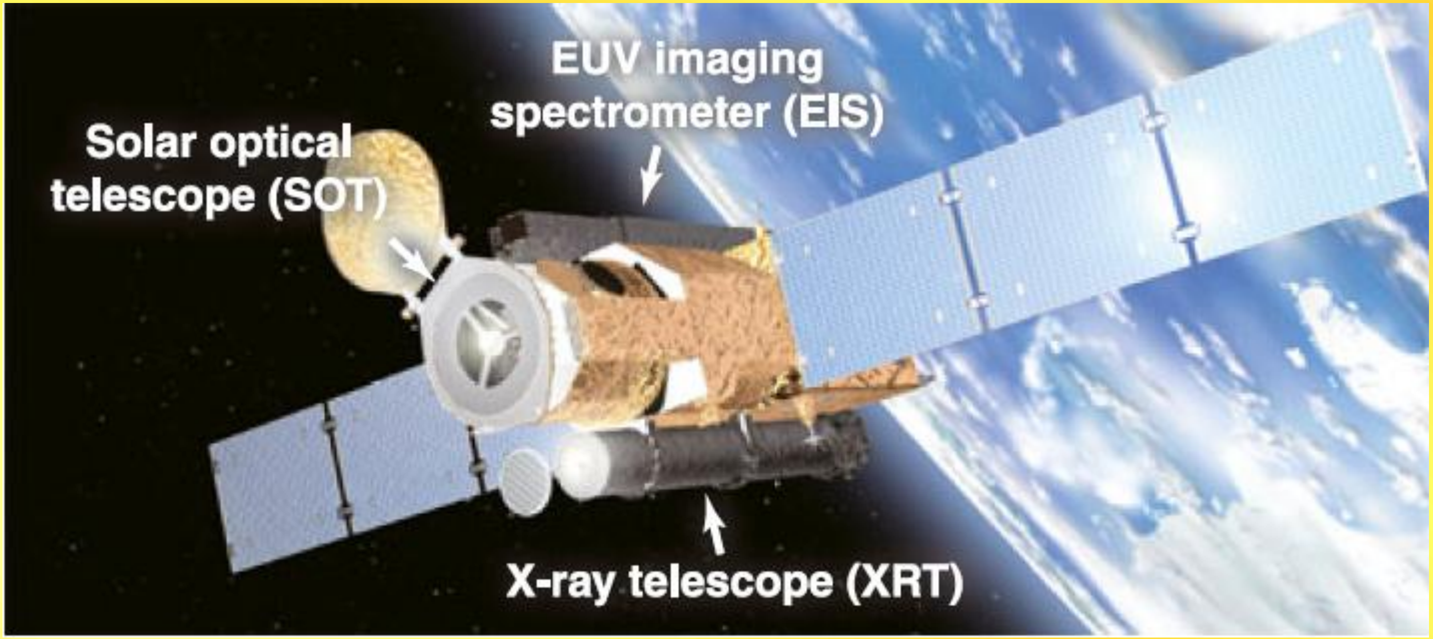

Narukage et al. (2011), Solar Phys. 269, 169

Hinode/XRT – filter wheels

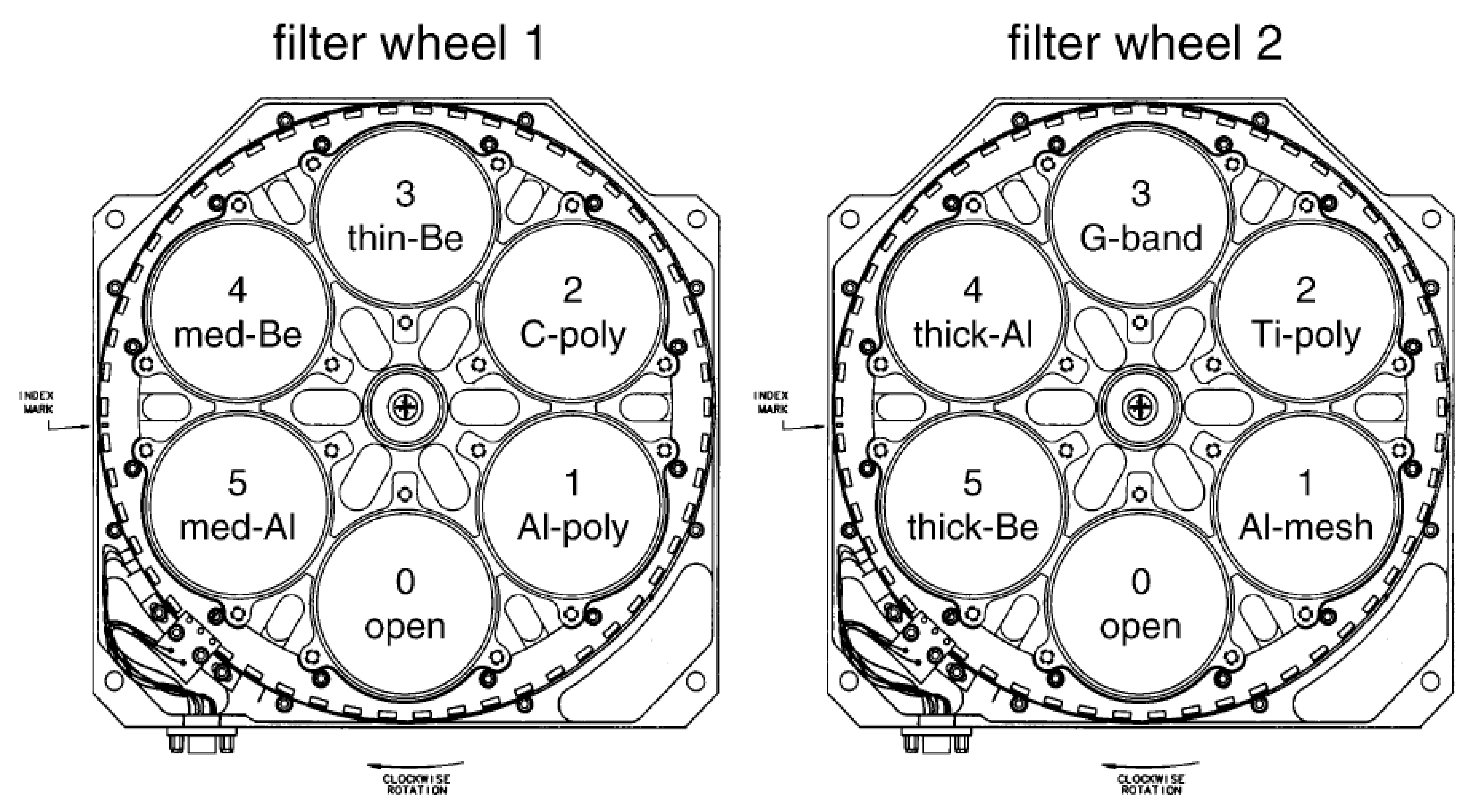

Narukage et al. (2011), Solar Phys. 269, 169

XRT – temperature response

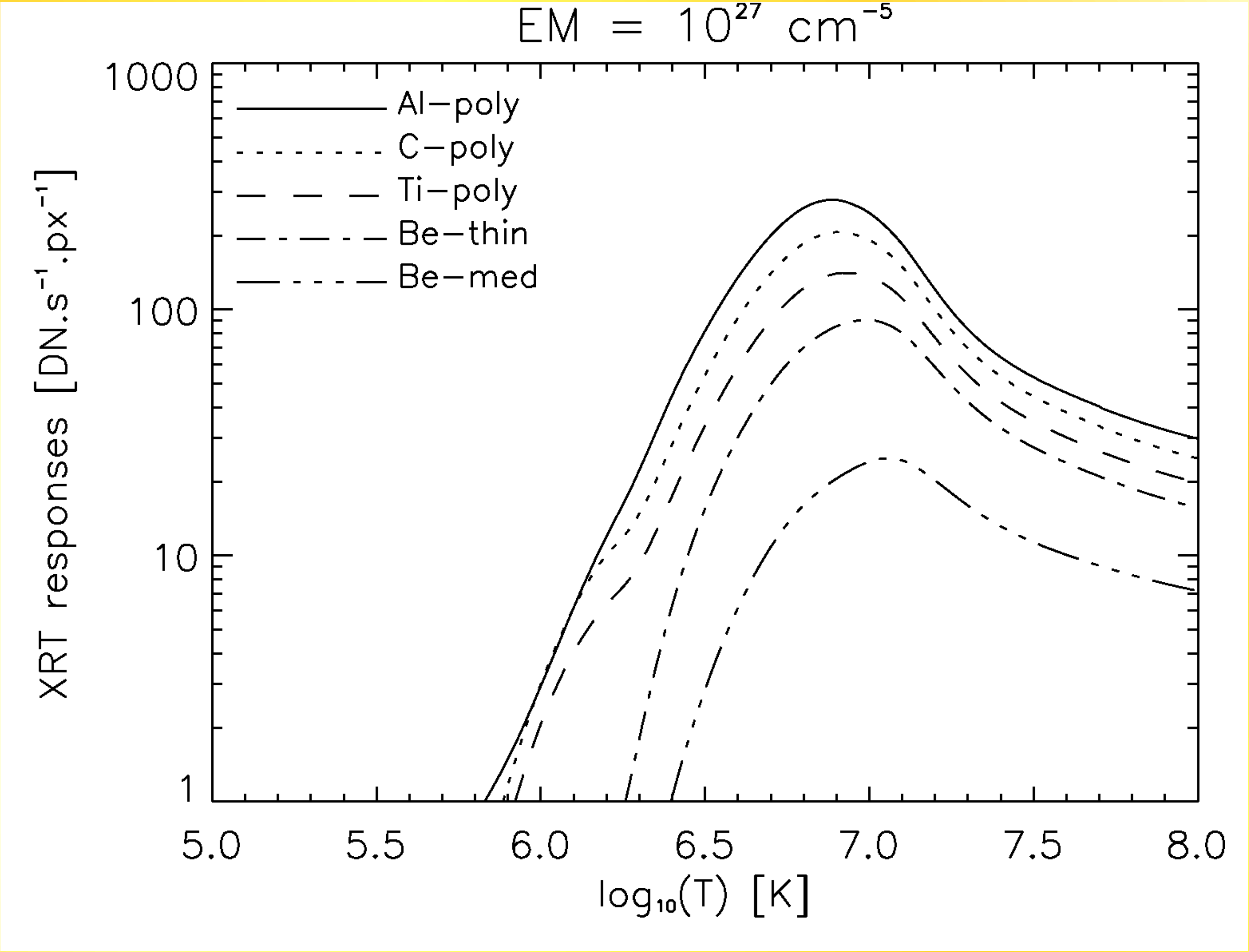

XRT – temperature diagnostic

$$CIFR(T) = \frac{\left(\prod_{i=1}^{5} F_i(T)\right)^{2/5}}{F_1(T)F_2(T)}$$

Reale et al. (2007)
Science 317, 1582

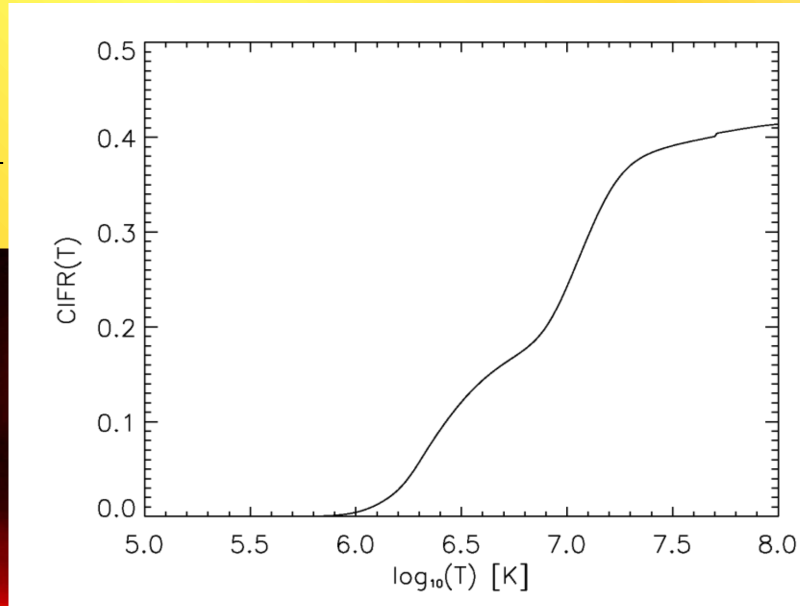

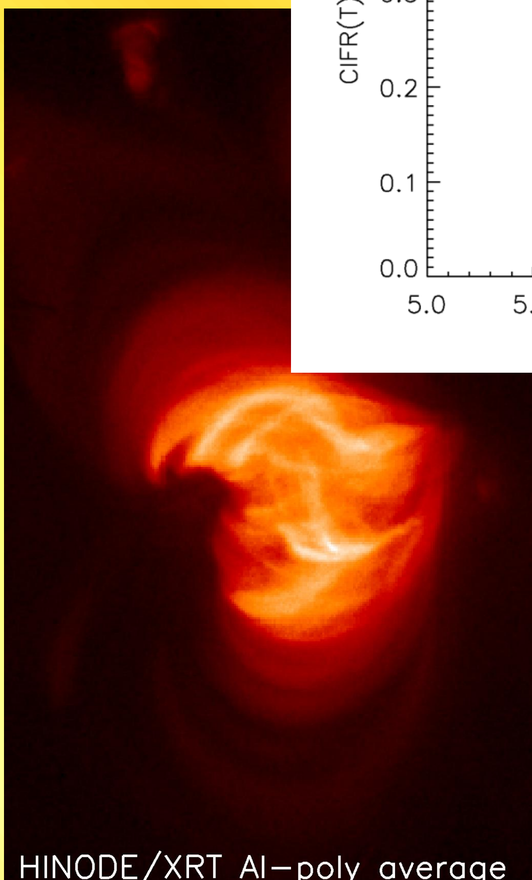

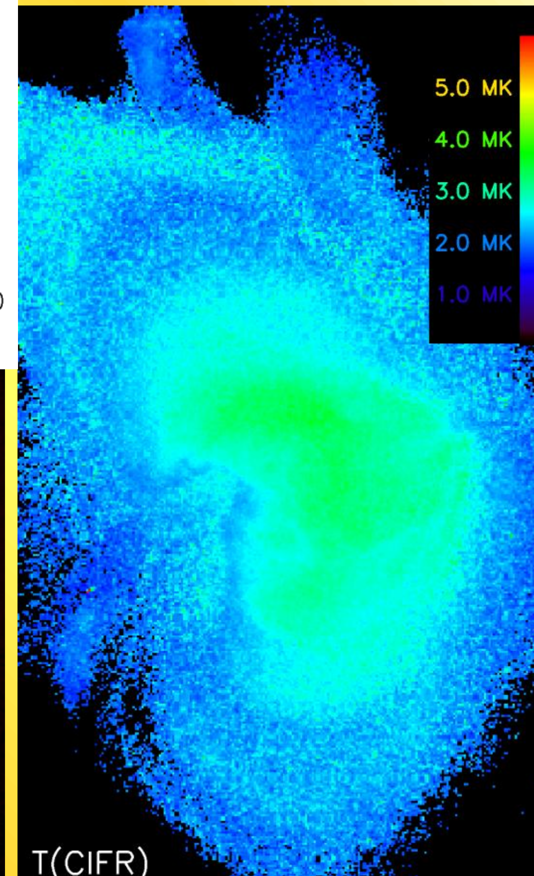

SDO/AIA

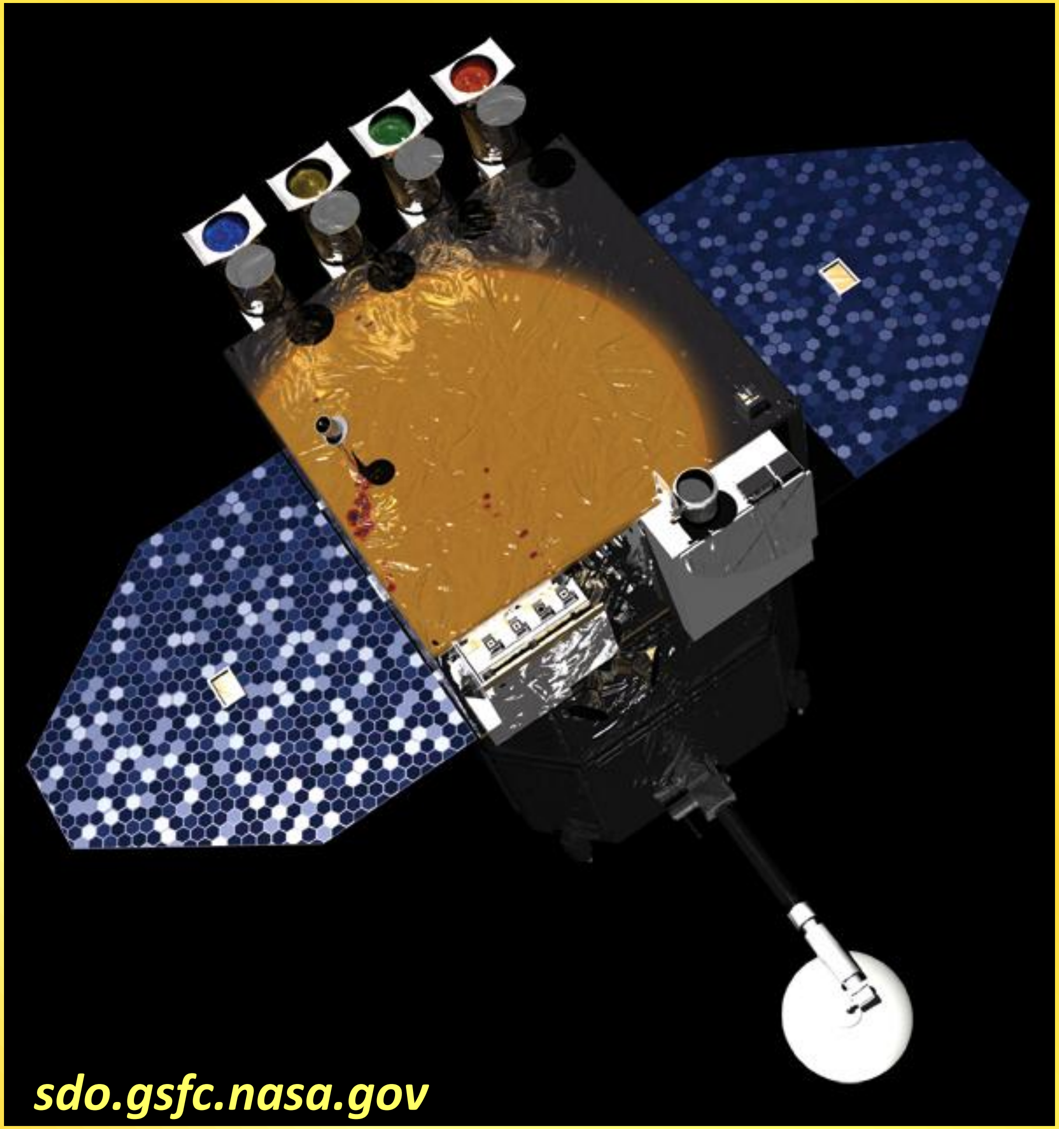

Solar Dynamics Observatory:
NASA mission, launched 2010

Atmospheric Imaging Assembly (AIA):
- four identical EUV full-disc telescopes, state-of-the-art
- cadence of few seconds
- 0.6” resolution
- broad temperature coverage
- successor to SoHO/EIT and TRACE

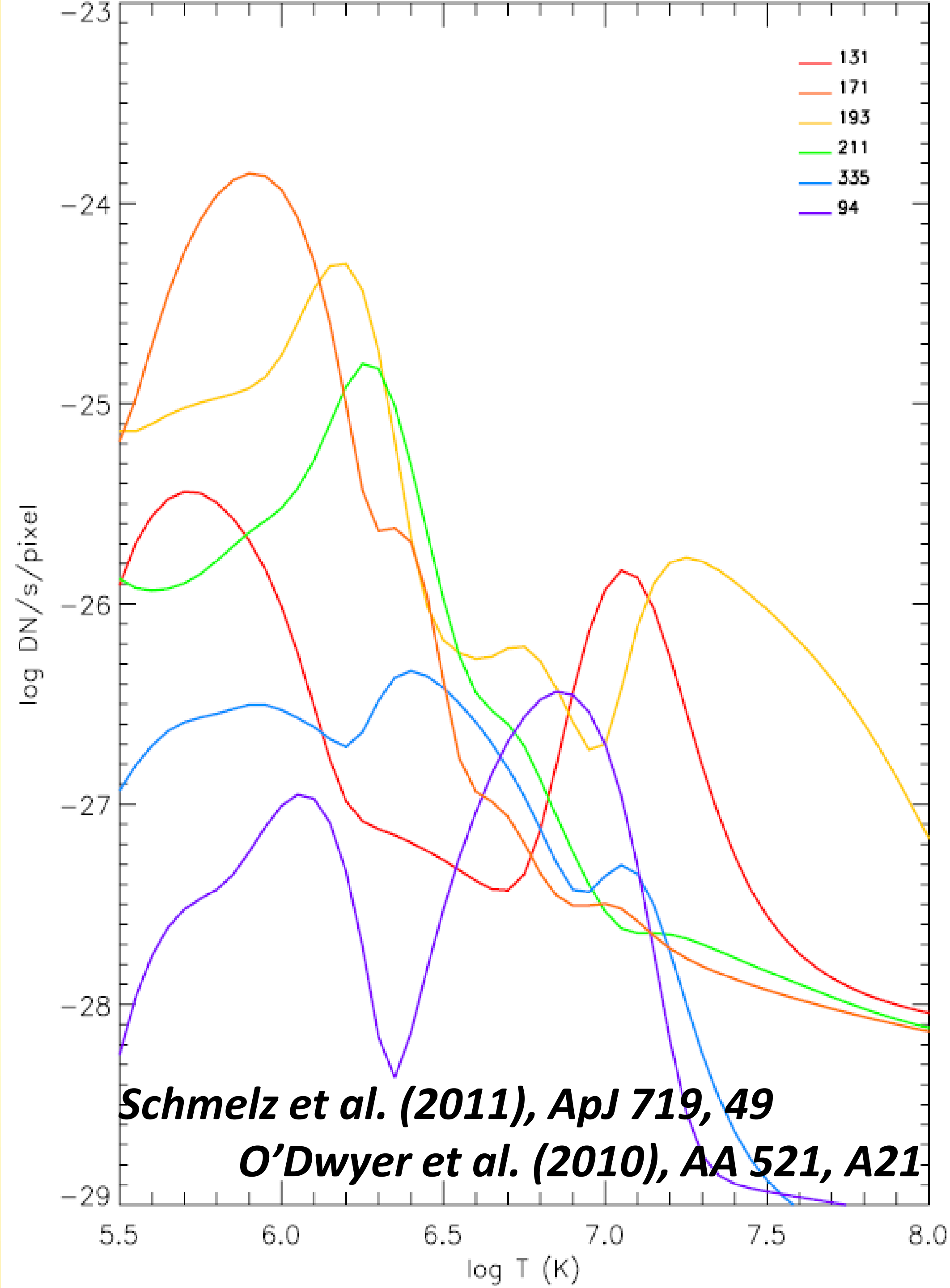

Table 1. Predicted AIA count rates.

	Ion	λ	T_p[a]	Fraction of total emission			
		Å	K	CH	QS	AR	FL
94 Å	Mg VIII	94.07	5.9	0.03	–	–	–
	Fe XX	93.78	7.0	–	–	–	0.10
	Fe XVIII	93.93	6.85	–	–	0.74	0.85
	Fe X	94.01	6.05	0.63	0.72	0.05	–
	Fe VIII	93.47	5.6	0.04	–	–	–
	Fe VIII	93.62	5.6	0.05	–	–	–
	Cont.			0.11	0.12	0.17	–
131 Å	O VI	129.87	5.45	0.04	0.05	–	–
	Fe XXIII	132.91	7.15	–	–	–	0.07
	Fe XXI	128.75	7.05	–	–	–	0.83
	Fe VIII	130.94	5.6	0.30	0.25	0.09	–
	Fe VIII	131.24	5.6	0.39	0.33	0.13	–
	Cont.			0.11	0.20	0.54	0.04
171 Å	Ni XIV	171.37	6.35	–	–	0.04	–
	Fe X	174.53	6.05	–	0.03	–	–
	Fe IX	171.07	5.85	0.95	0.92	0.80	0.54
	Cont.			–	–	–	0.23
193 Å	O V	192.90	5.35	0.03	–	–	–
	Ca XVII	192.85	6.75	–	–	–	0.08
	Ca XIV	193.87	6.55	–	–	0.04	–
	Fe XXIV	192.03	7.25	–	–	-	0.81
	Fe XII	195.12	6.2	0.08	0.18	0.17	–
	Fe XII	193.51	6.2	0.09	0.19	0.17	–
	Fe XII	192.39	6.2	0.04	0.09	0.08	–
	Fe XI	188.23	6.15	0.09	0.10	0.04	–
	Fe XI	192.83	6.15	0.05	0.06	–	–
	Fe XI	188.30	6.15	0.04	0.04	–	–
	Fe X	190.04	6.05	0.06	0.04	–	–
	Fe IX	189.94	5.85	0.06	–	–	–
	Fe IX	188.50	5.85	0.07	–	–	–
	Cont.			–	–	0.05	0.04
211 Å	Cr IX	210.61	5.95	0.07	–	–	–
	Ca XVI	208.60	6.7	–	–	–	0.09
	Fe XVII	204.67	6.6	–	–	–	0.07
	Fe XIV	211.32	6.3	–	0.13	0.39	0.12
	Fe XIII	202.04	6.25	–	0.05	–	–
	Fe XIII	203.83	6.25	–	–	0.07	–

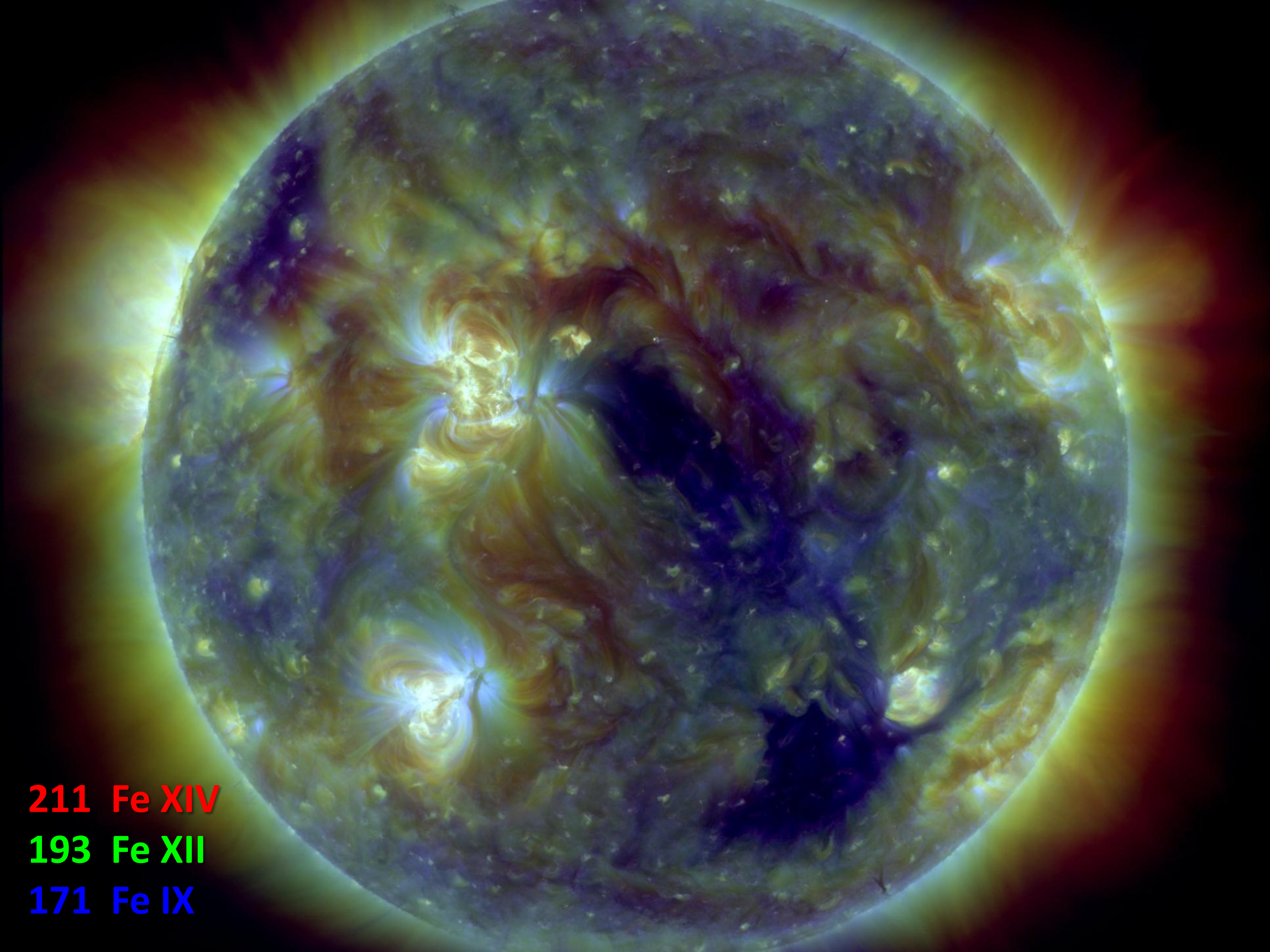
211 Fe XIV
193 Fe XII
171 Fe IX

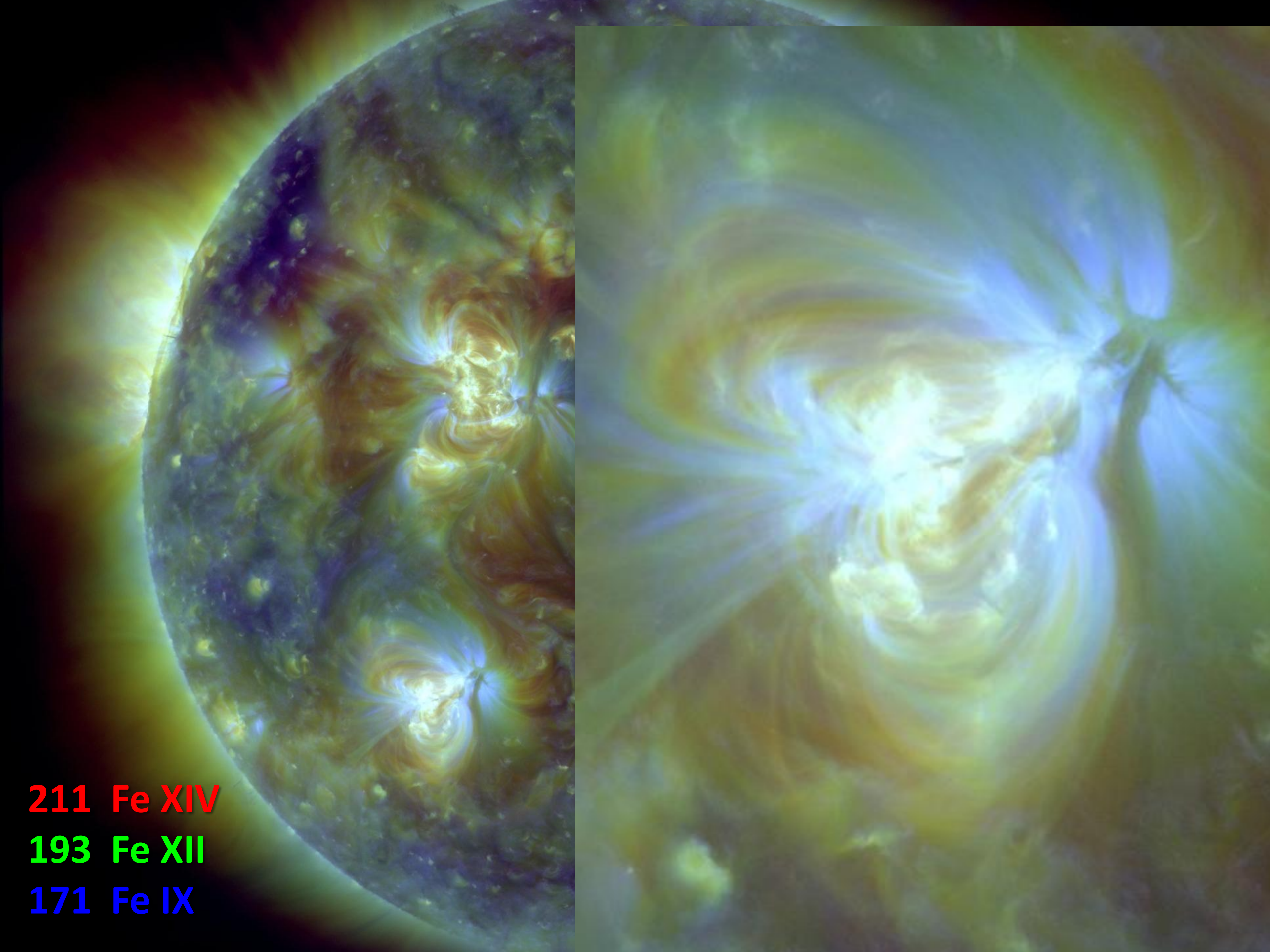
211 Fe XIV
193 Fe XII
171 Fe IX

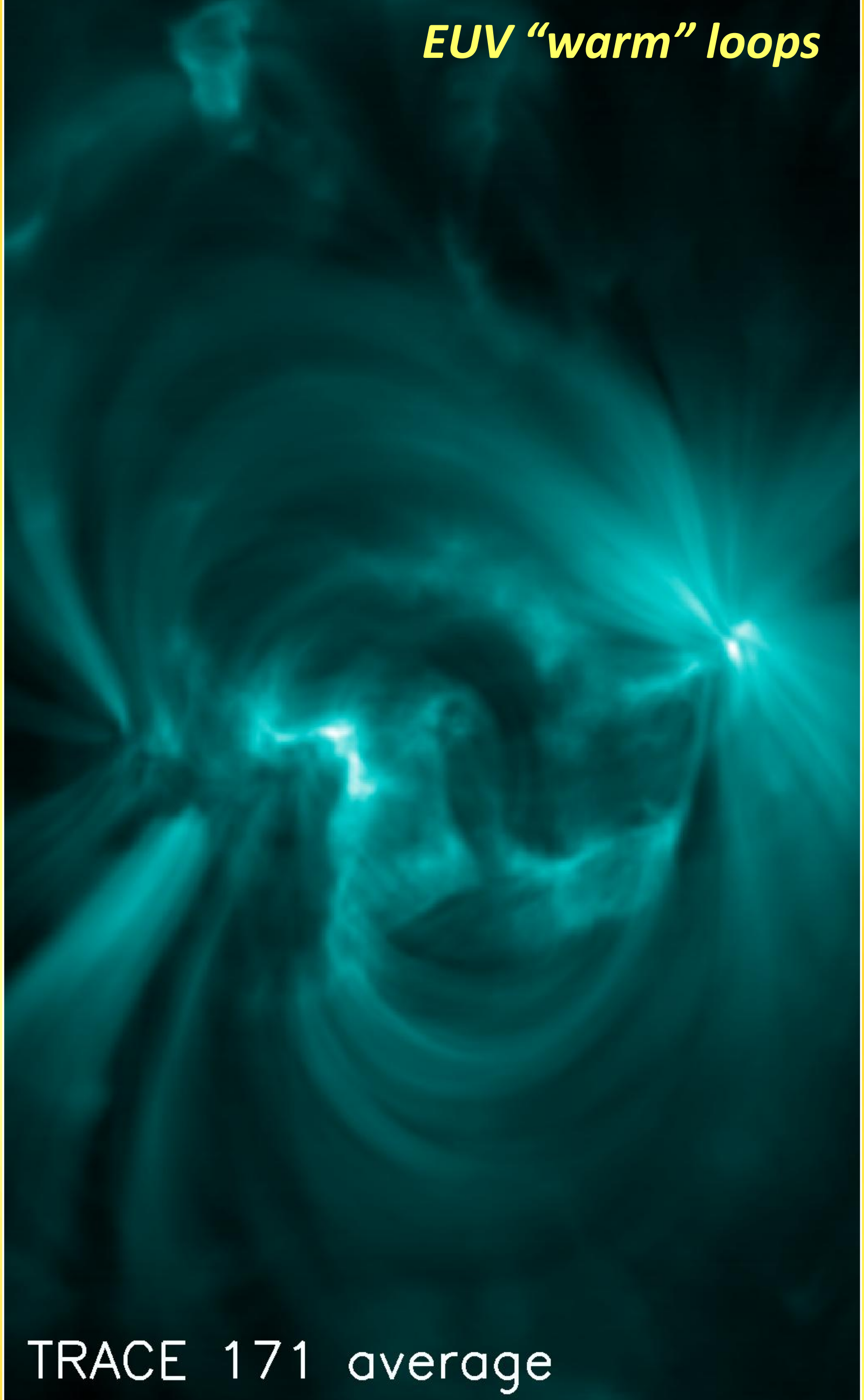
EUV "warm" loops
TRACE 171 average

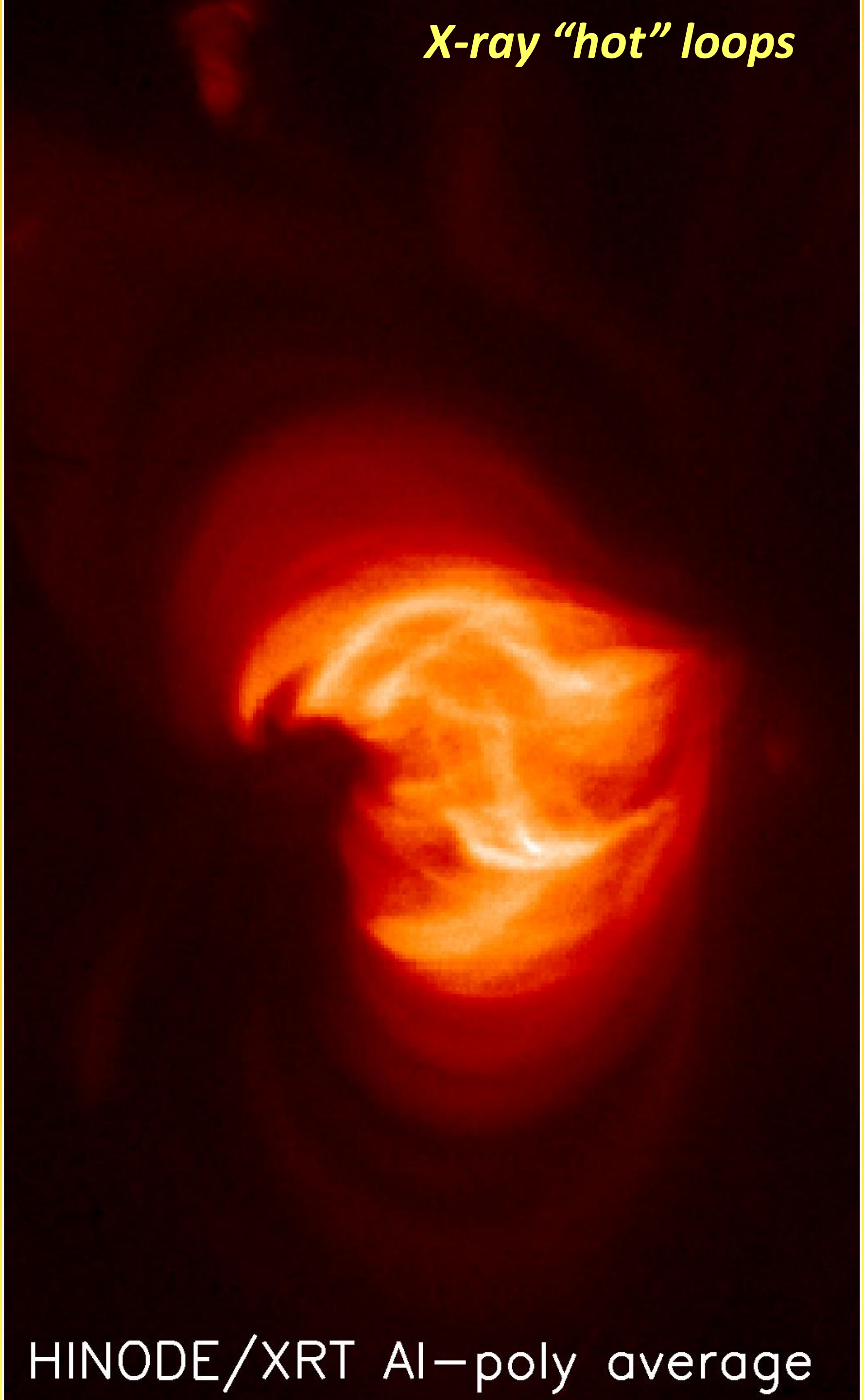
X-ray "hot" loops
HINODE/XRT Al-poly average

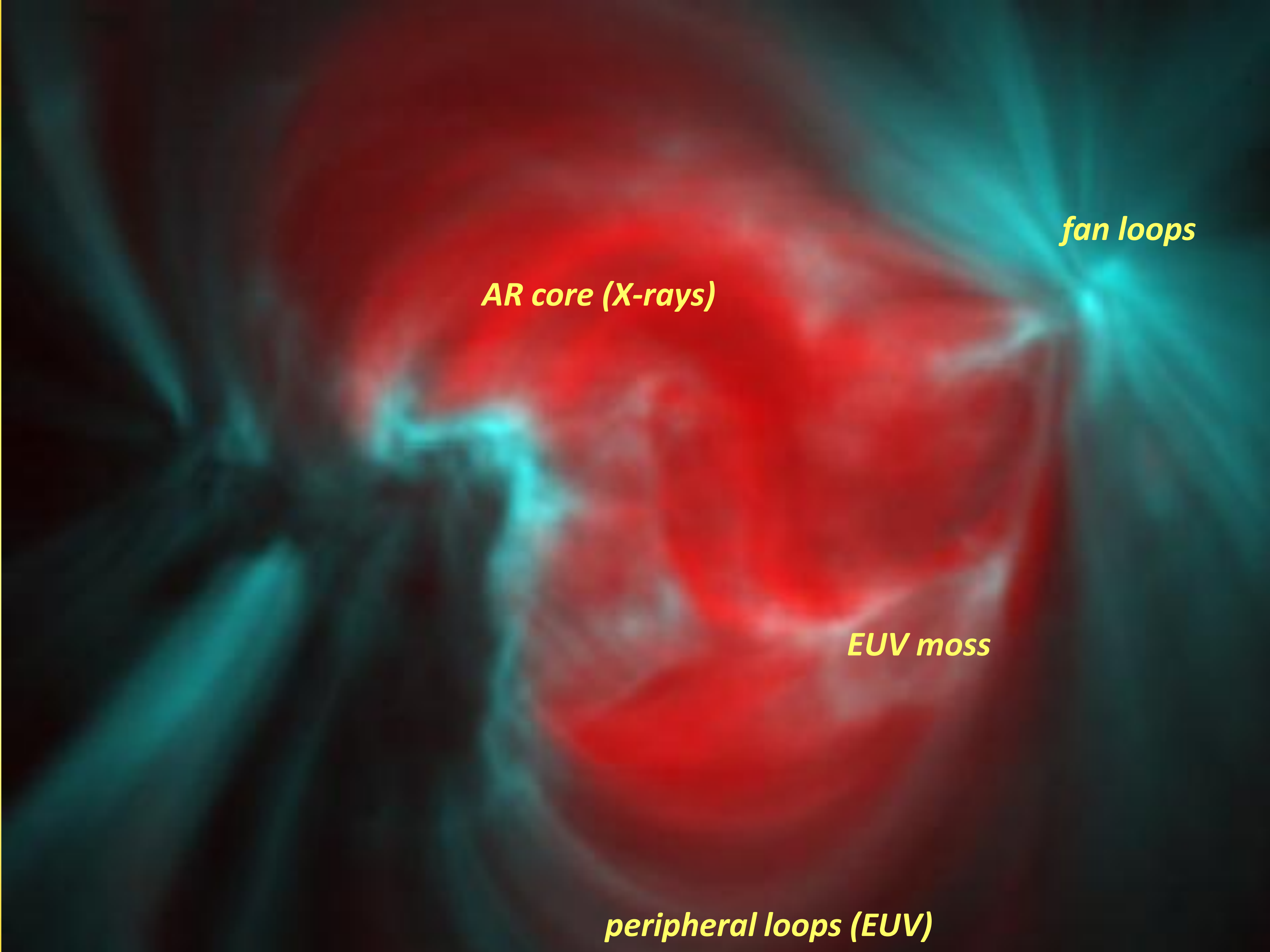
fan loops
AR core (X-rays)
EUV moss
peripheral loops (EUV)

TRACE 171 warm loops

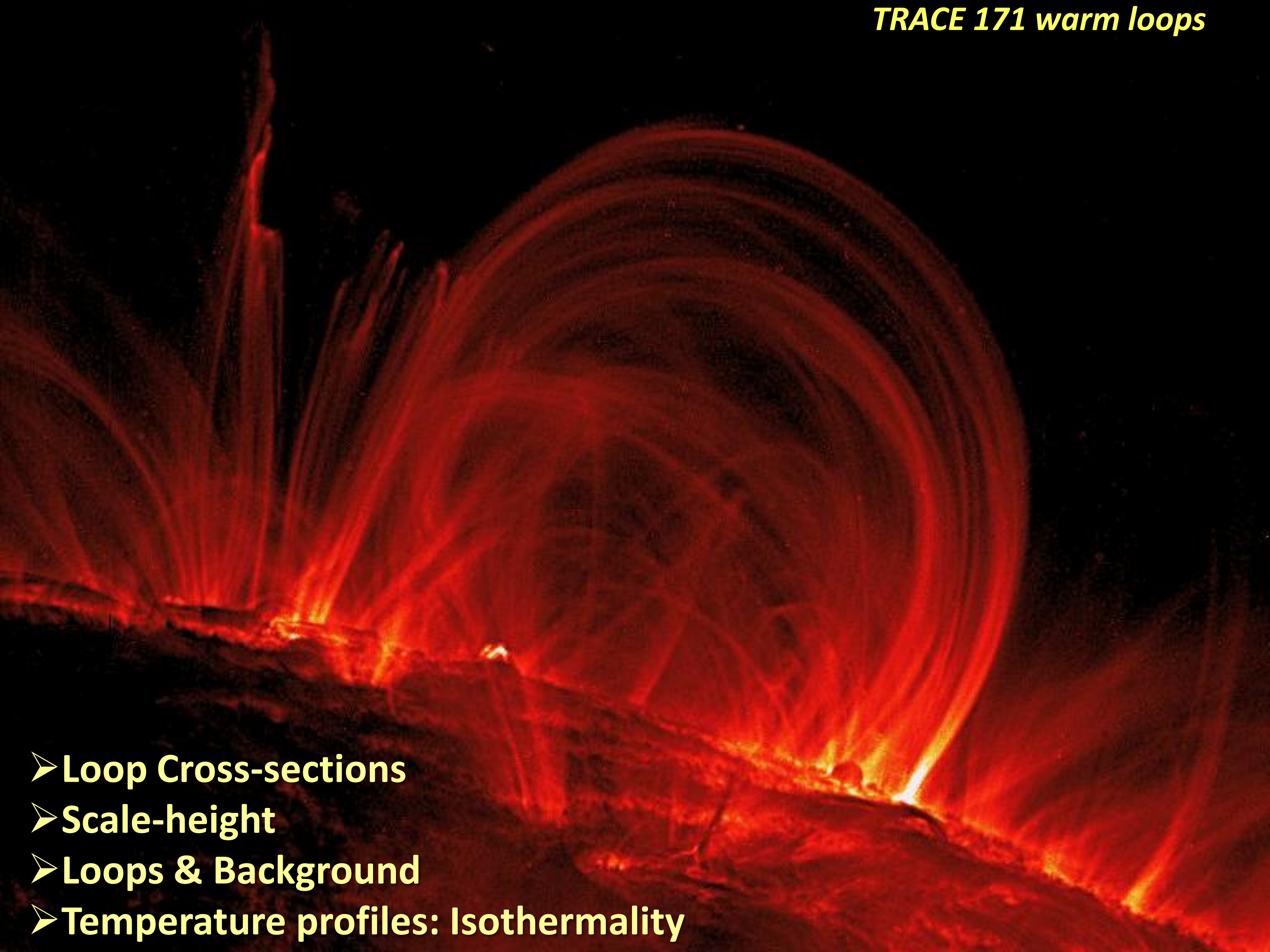

- Loop Cross-sections
- Scale-height
- Loops & Background
- Temperature profiles: Isothermality

Loops - geometry

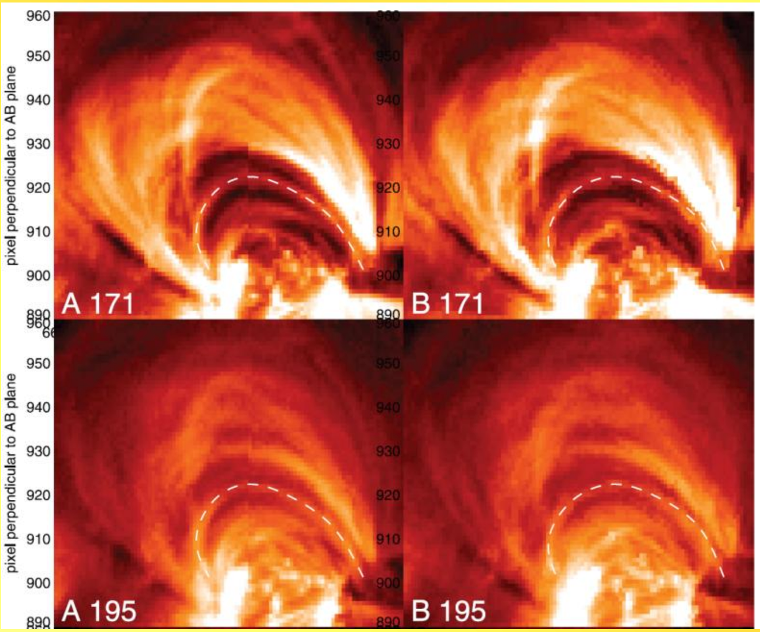

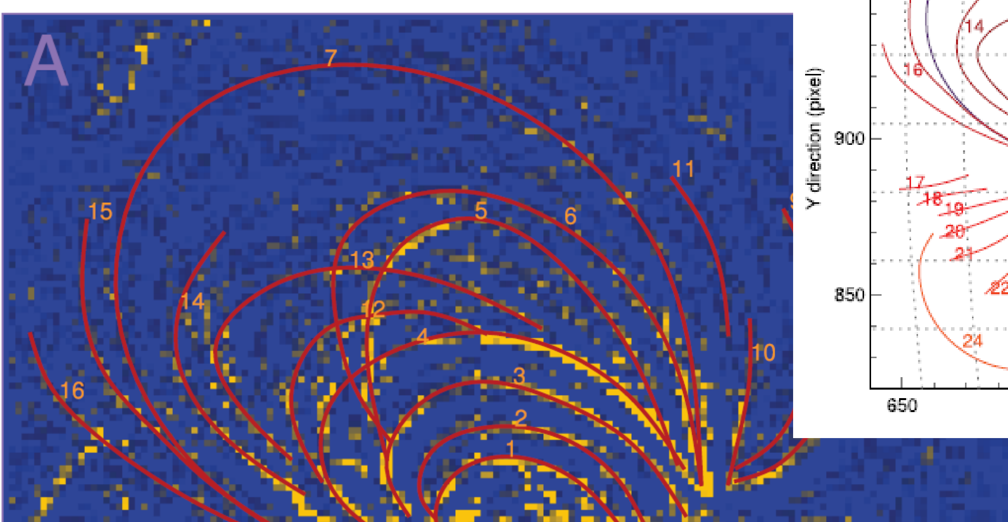

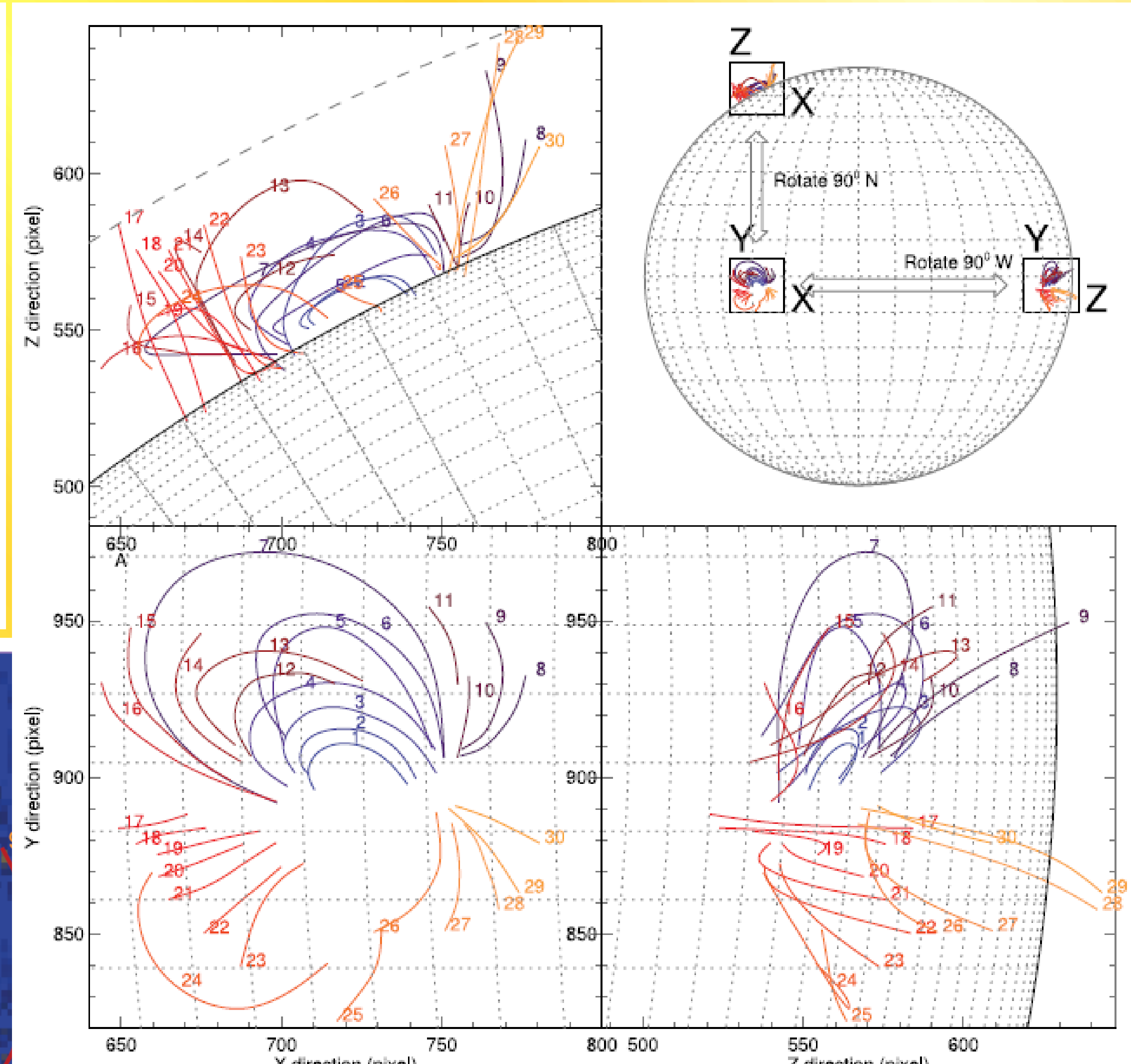

Aschwanden et al. (2008), ApJ 679, 827

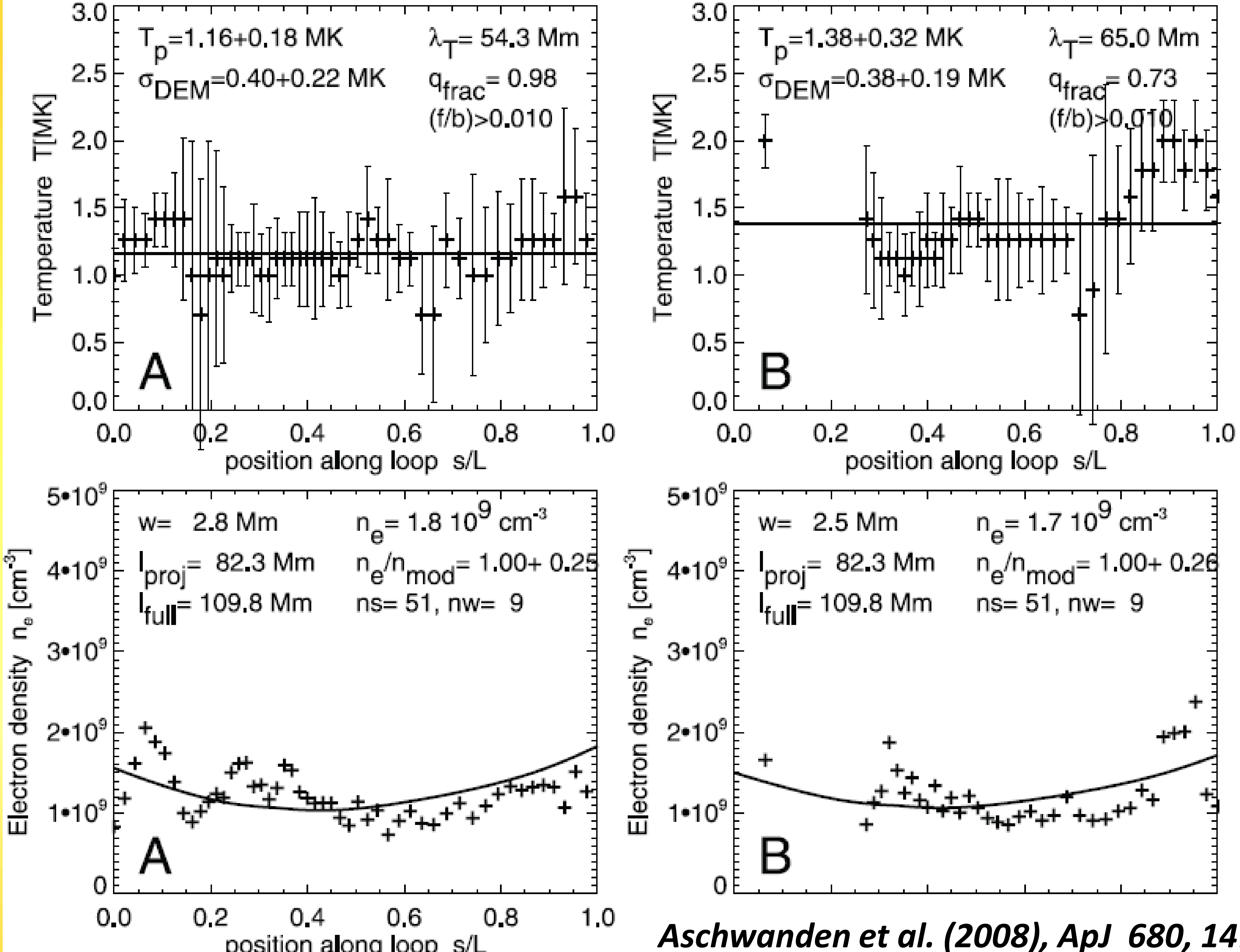

Aschwanden et al. (2008), ApJ 680, 1477

Loops can be hydrostatic

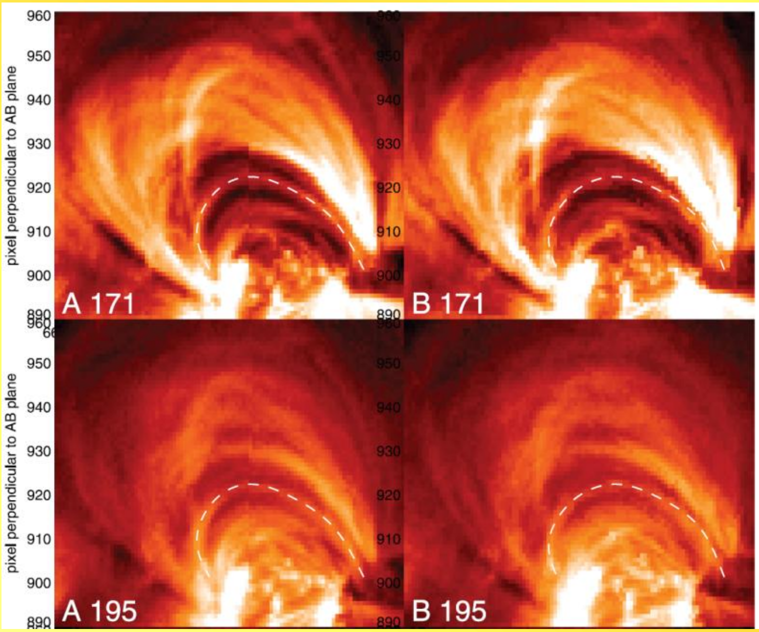

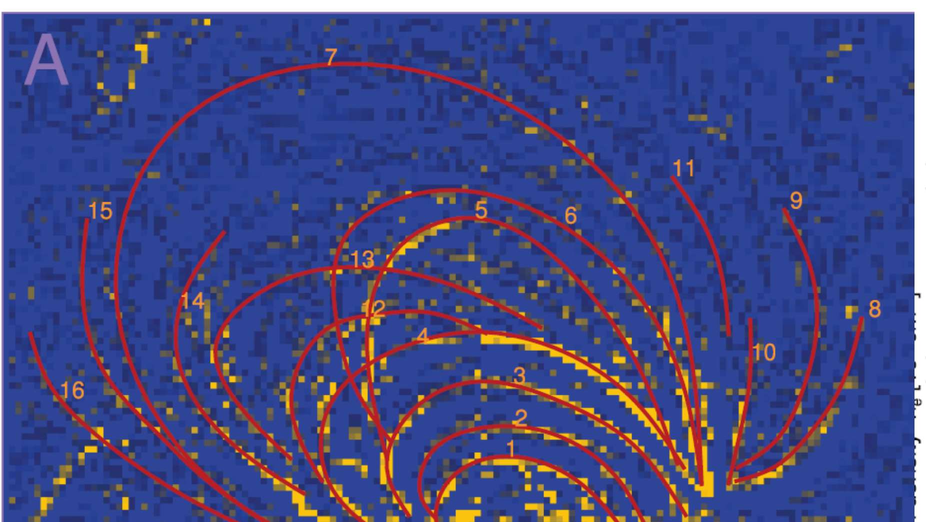

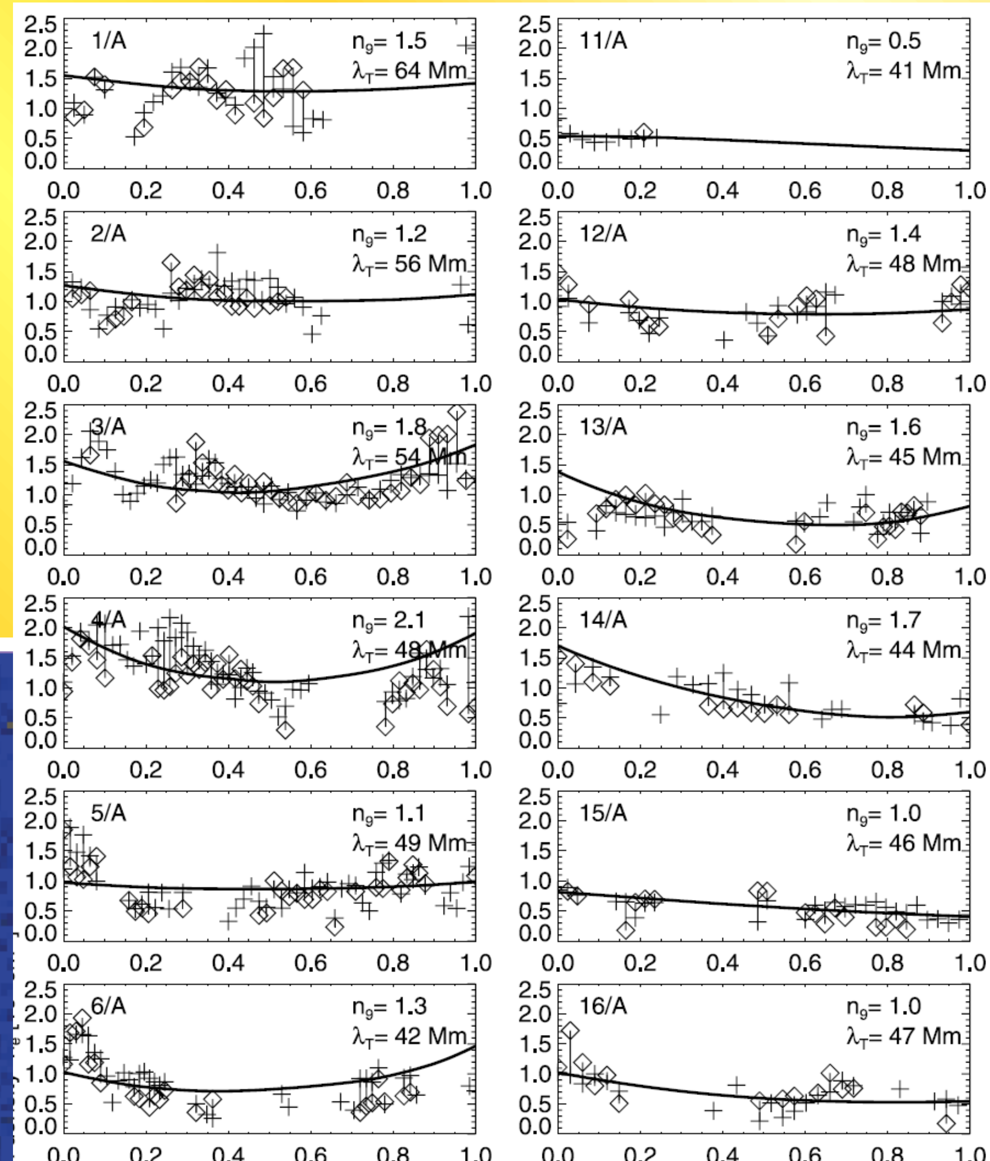

WARNING: BACKGROUND !

Background can be ~ 80% of the actual observed signal:

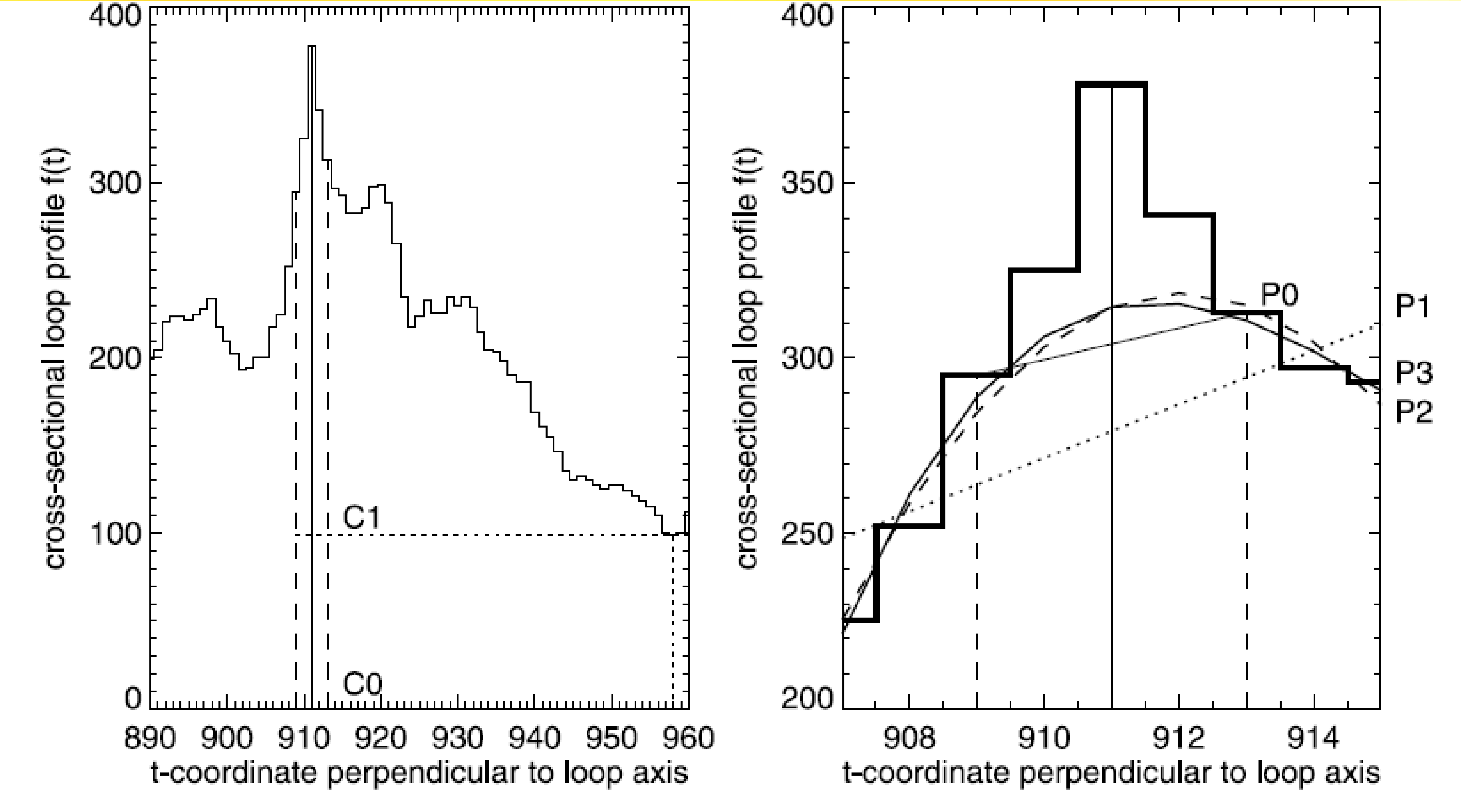

Aschwanden et al. (2008), ApJ 680, 1477

Loops or strands…

Aschwanden et al. (2000), ApJ 541, 1059

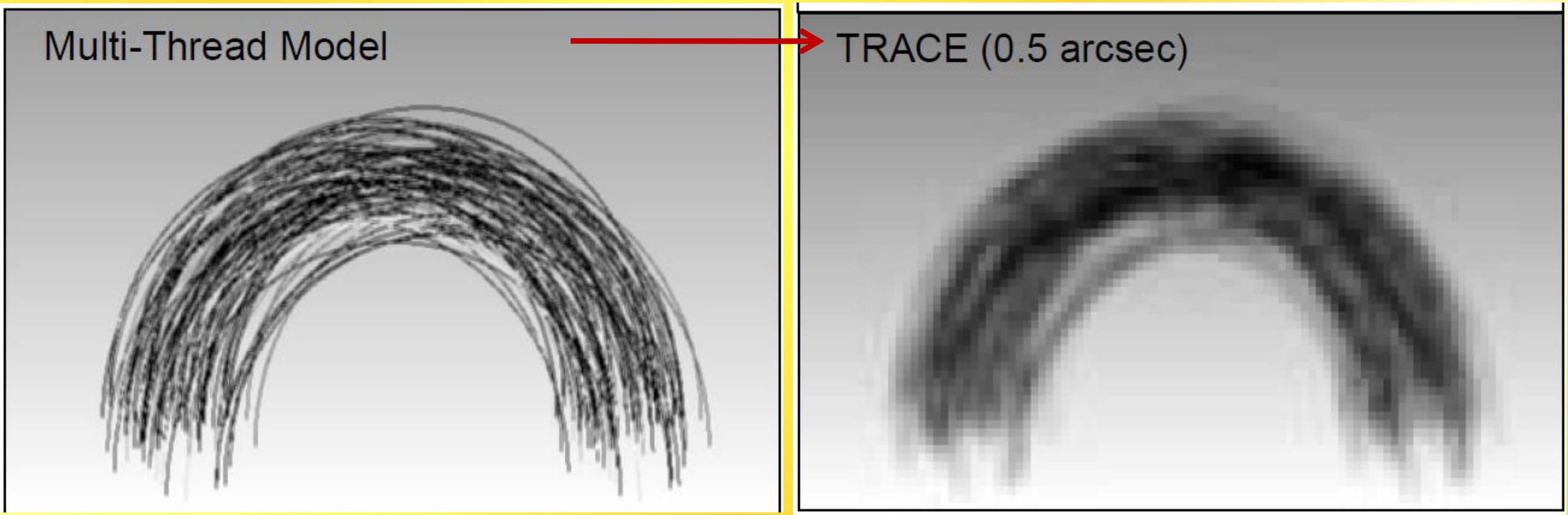

Loop: coherent structure in an observed image of the corona
Strand: Fundamental, independent, elementary structure with an isothermal cross-field profile, thickness down to the gyro-radius < 1 m

Reale & Peres (2000), ApJ 521, L45: *Multithermal, multi-strand loop, with different temperature structure for each strand, can produce false "isothermal" loop if unresolved*

Isothermal or multithermal?

***Schmelz et al. (2009): ApJ 691, 503:** Are Coronal Loops Isothermal or Multithermal?*

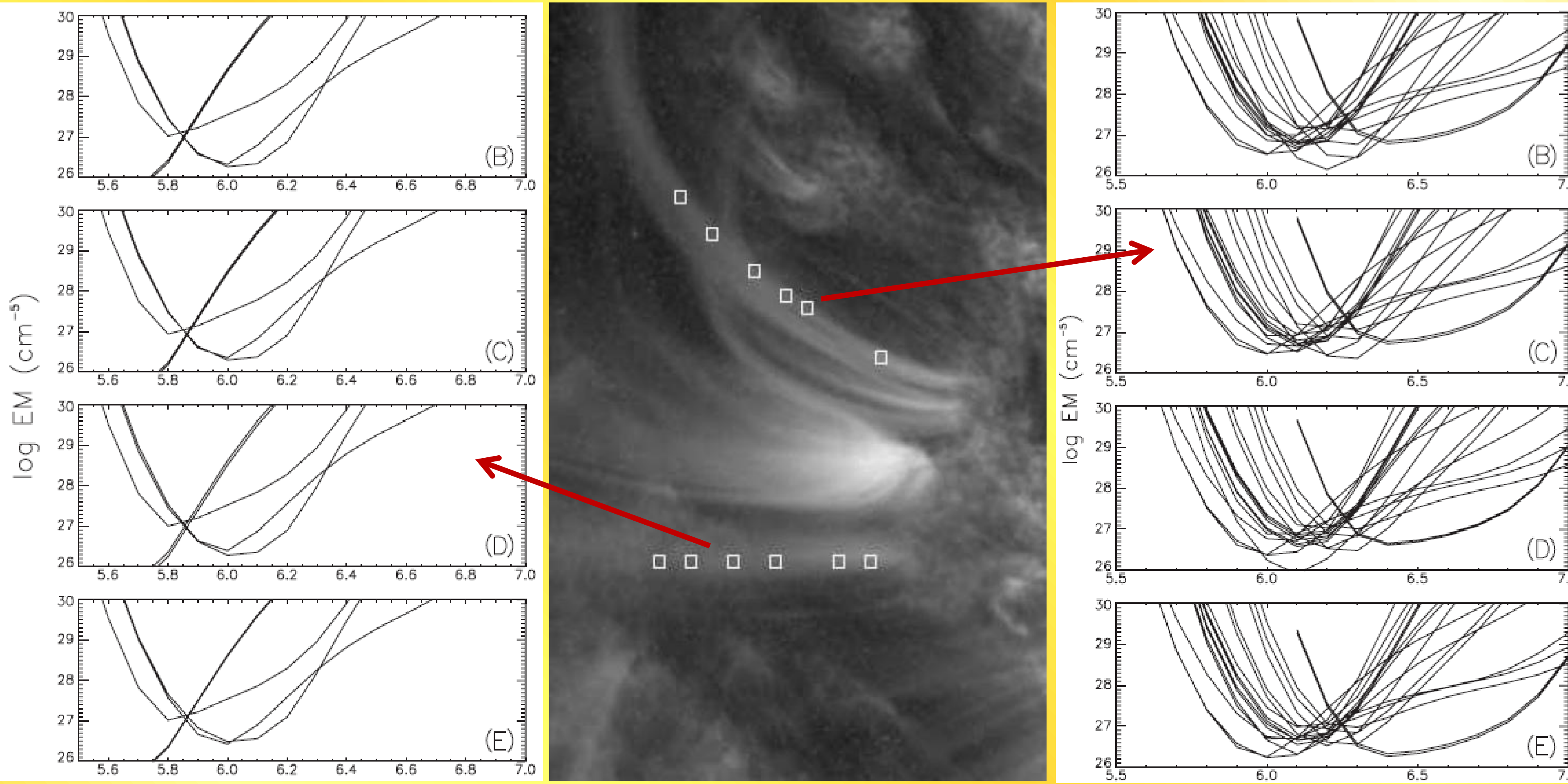

Conclusion: Yes

Loop dynamics

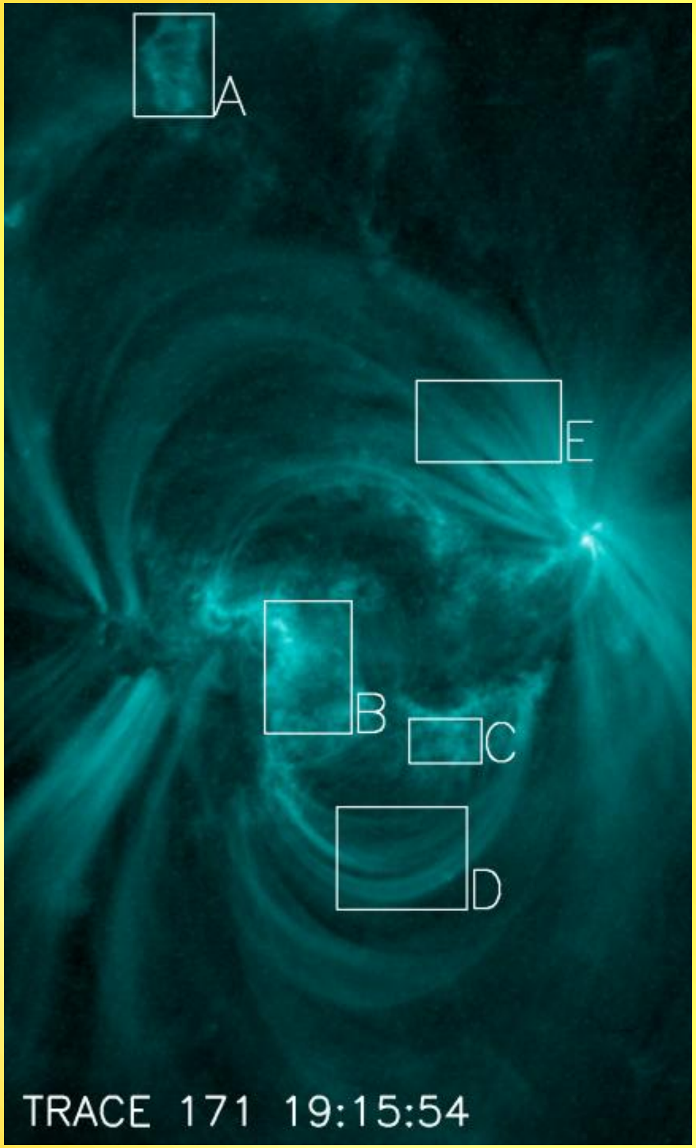

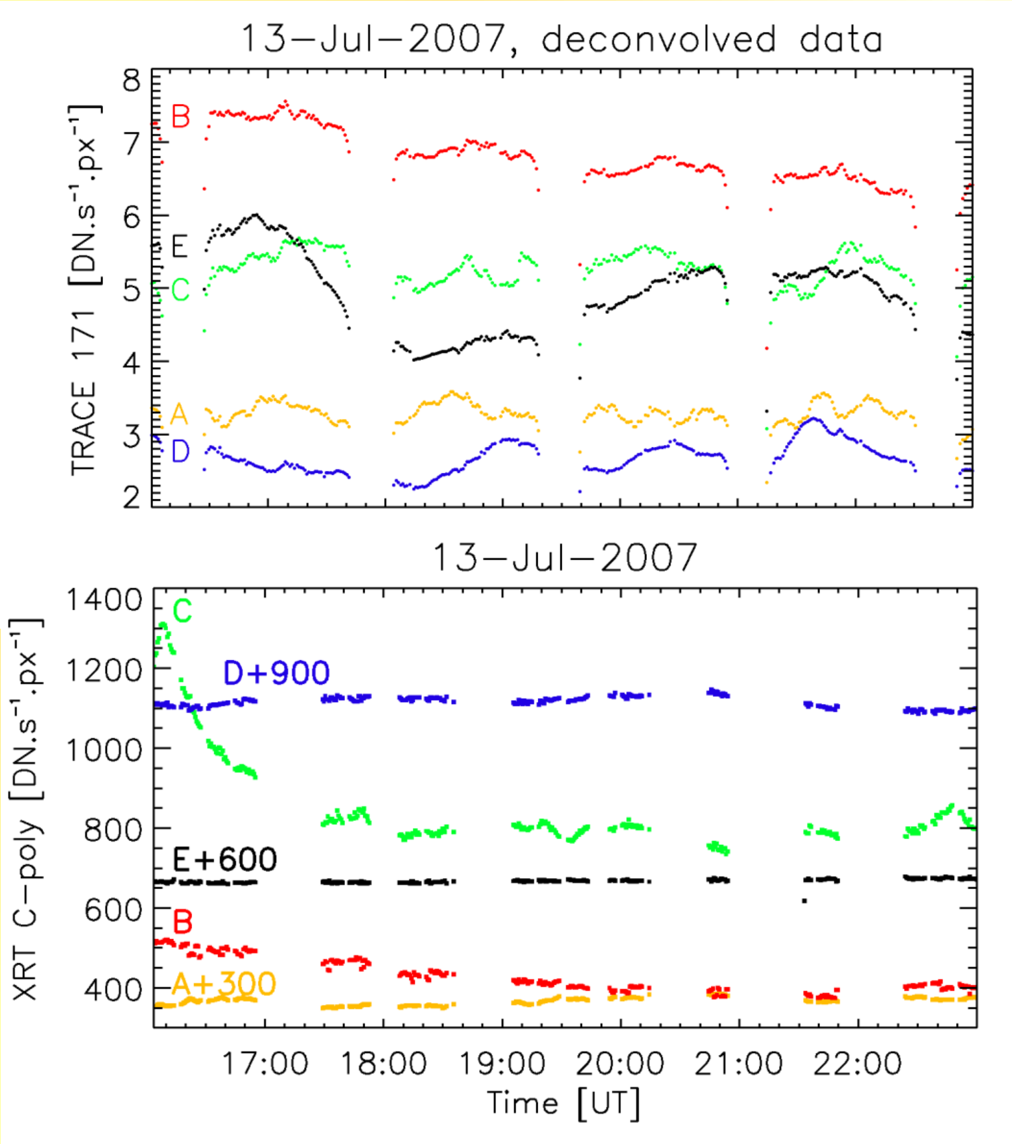

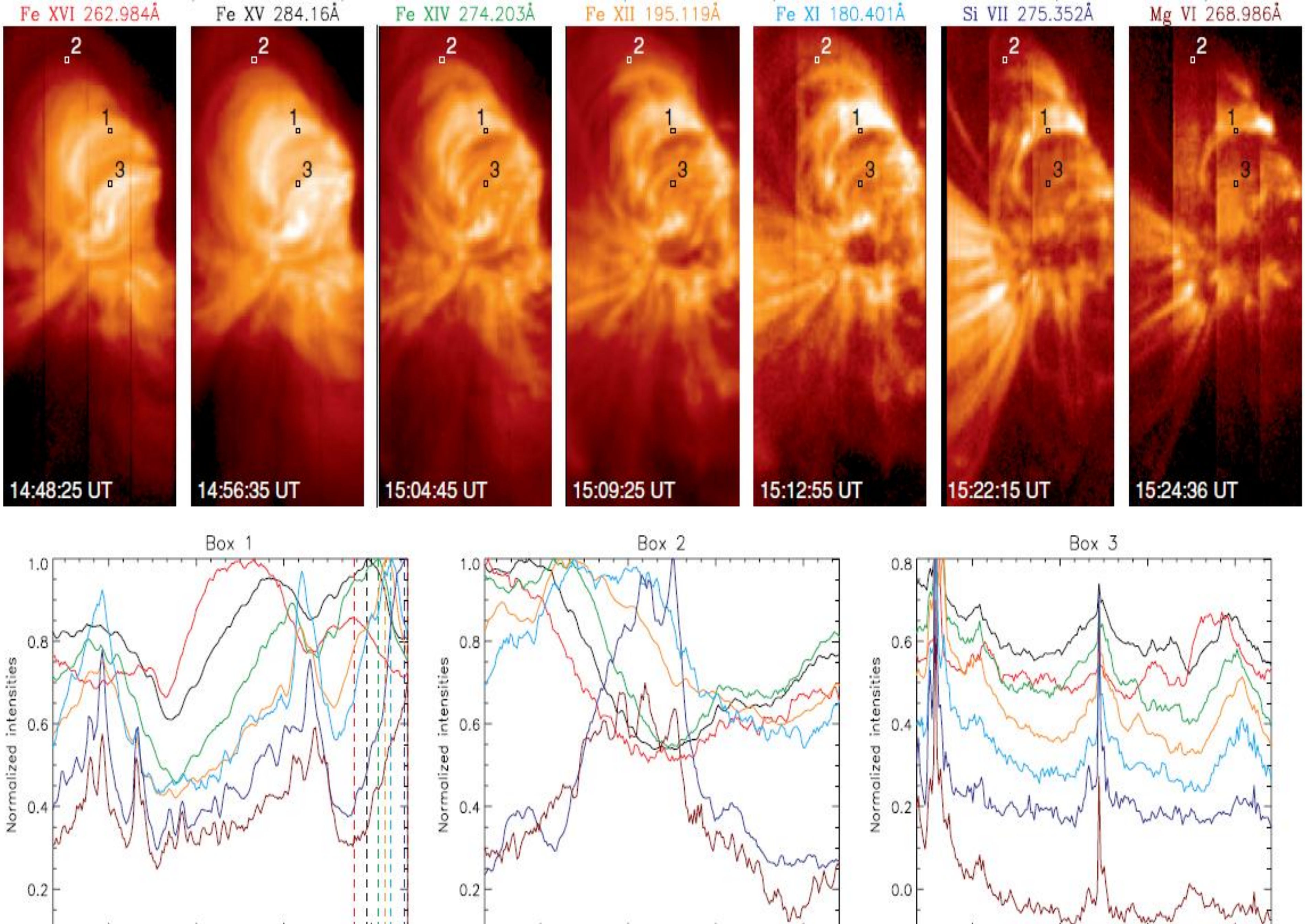

Ugarte-Urra et al. (2009), ApJ 695, 642

The Coronal Heating Problem

- The Corona is heated to temperatures of several MK. **But how?**
- Small-scale reconnection:
  Parker's nanoflares
- Wave heating
- <u>Note on terminology:</u>
  The current "nanoflare" models simply refer to any impulsive energy release
  (papers by the Klimchuk group)

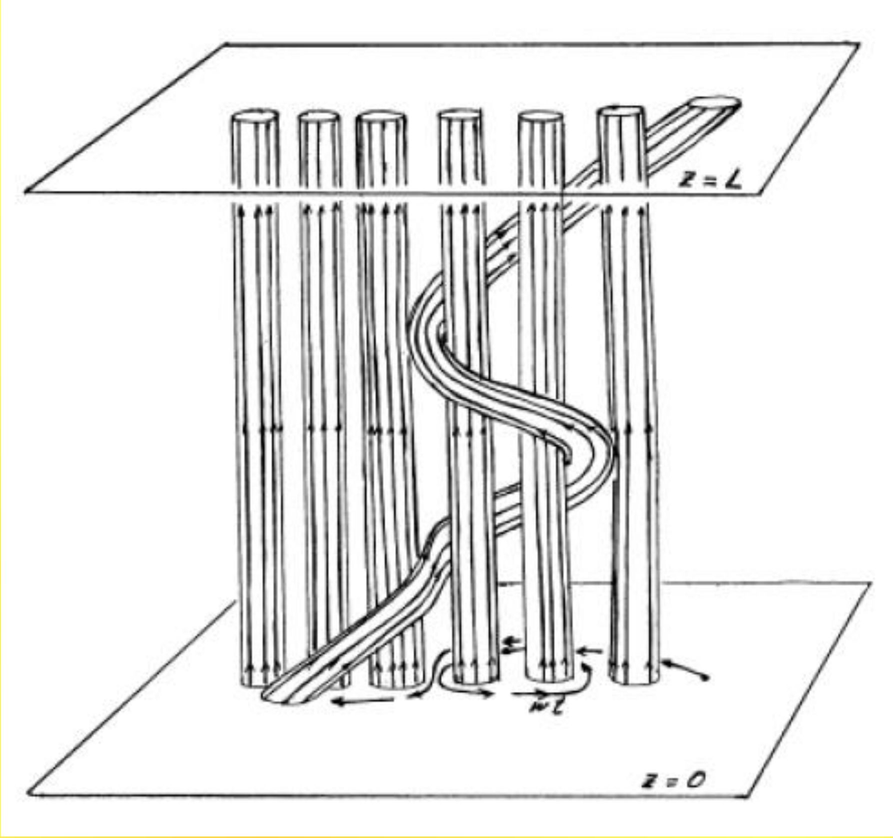

Required heating flux

Exponentially decreasing heating

$$F_{\mathrm{H}} = E_{\mathrm{H0}} s_{\mathrm{H}}$$

$$\approx 5\times10^{3}\left(\frac{n_e}{10^{8}\,\mathrm{cm}^{-3}}\right)^{2}\left(\frac{T}{1\ \mathrm{MK}}\right)\quad [\mathrm{ergs\ cm^{-2}s^{-1}}]$$

$$\uparrow$$

$$E_{\mathrm{H0}} \approx E_{rad} = n_e^2 Q(T)$$

- **Coronal hole:** $T \approx 1$ MK, $n_e \approx 10^{8}$ cm^{-3} : $F_{\mathrm{H}} \approx 5\ \mathrm{x}10^{3}$ ergs cm^{-2} s^{-1}
- **Active region:** $T \approx 2.5$ MK, $n_e \approx 2\ \mathrm{x}10^{9}$ cm^{-3} : $F_{\mathrm{H}} \approx 5\ \mathrm{x}10^{6}$ ergs cm^{-2}

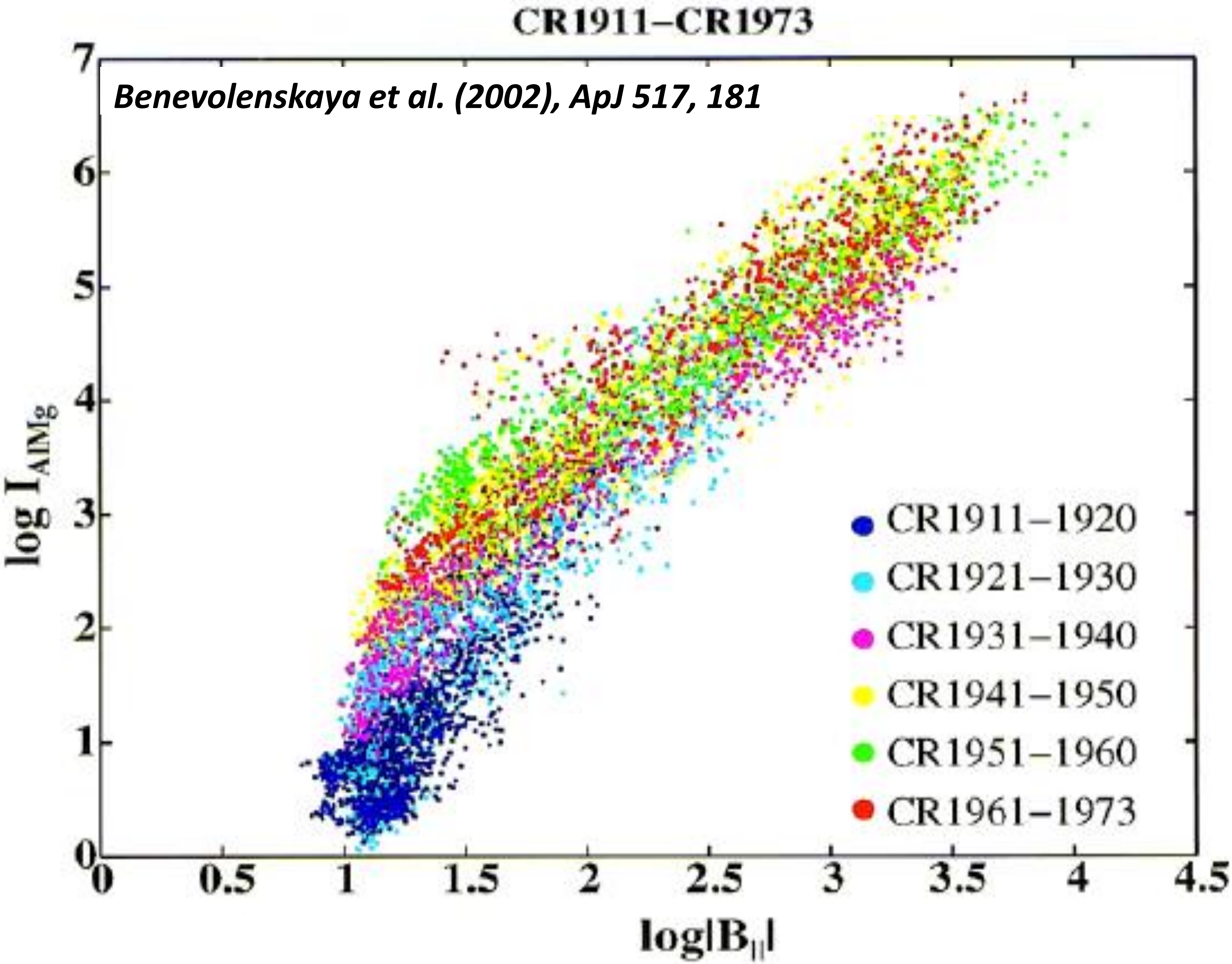

CR1911–CR1973
Benevolenskaya et al. (2002), ApJ 517, 181
log I$_{AIMg}$
log|B$_{||}$|
CR1911–1920
CR1921–1930
CR1931–1940
CR1941–1950
CR1951–1960
CR1961–1973

Modeling: MHD Equations

$$\rho\left(\frac{\partial\vec{v}}{\partial t}+\left(\vec{v}.\vec{\nabla}\right)\vec{v}\right)=-\vec{\nabla}p_{\mathrm{G}}+\vec{j}\times\vec{B}+\rho\vec{g},$$

$$\frac{1}{\gamma-1}\left(\frac{\partial T}{\partial t}+\vec{v}.\vec{\nabla}T\right)=-T\vec{\nabla}.\vec{v}+\frac{1}{qk_{\mathrm{B}}n_{\mathrm{e}}}\left(E_{\mathrm{H}}-n_{\mathrm{e}}^{2}Q(T)+\vec{\nabla}.\vec{F}_{\mathrm{C}}\right),$$

$$\frac{\partial\vec{B}}{\partial t}=\vec{\nabla}\times\left(\vec{v}\times\vec{B}\right),$$

$$\frac{\partial\rho}{\partial t}+\vec{\nabla}.\left(\rho\vec{v}\right)=0, \qquad \vec{j}=\frac{1}{\mu}\vec{\nabla}\times\vec{B},$$

$$\vec{\nabla}.\vec{B}=0, \qquad p=qn_{\mathrm{e}}k_{\mathrm{B}}T=\frac{\rho k_{\mathrm{B}}T}{\bar{\mu}m_{\mathrm{H}}},$$

$$F_{\mathrm{C},\|}=\kappa_{0}T^{5/2}\frac{dT}{ds}, \qquad F_{\mathrm{C},\perp}=0.$$

Simple solution: Scaling laws

Assumptions:

- No time derivatives
- No flows
- Geometrically symmetric loop with symmetric heating
- Vanishing thermal conductivity at loop apex and footpoints

Rosner, Tucker, Vaiana (1978)
Serio et al. (1981)
Aschwanden & Schrijver (2002)
Dudík et al. (2009)
Martens (2010)

$$p_0\left(L_0, s_\mathrm{H}, T_1\right) = L_0^{-1} T_1^{3} S_1^{-3},$$

$$E_\mathrm{H0}\left(L_0, s_\mathrm{H}, T_1\right) = L_0^{-2} T_1^{7/2} S_2,$$

$$S_1^\mathrm{RTV} = 1{,}4 \times 10^{2} \quad [\mathrm{K\ s^{2/3} kg^{-1/3}}],$$

$$S_2^\mathrm{RTV} = 9{,}5 \times 10^{-6} \quad [\mathrm{kg\ m\ s^{-3} K^{-7/2}}].$$

$$S_1^\mathrm{Serio} = 1.4 \times 10^{2}\ \mathrm{e}^{-\left(0{,}08\, L_0/s_\mathrm{H} + 0{,}04\, L_0/s_p\right)},$$

$$S_2^\mathrm{Serio} = 9{,}5 \times 10^{-6}\ \mathrm{e}^{\left(0{,}78\, L_0/s_\mathrm{H} - 0{,}36\, L_0/s_p\right)}.$$

Comparison to observations

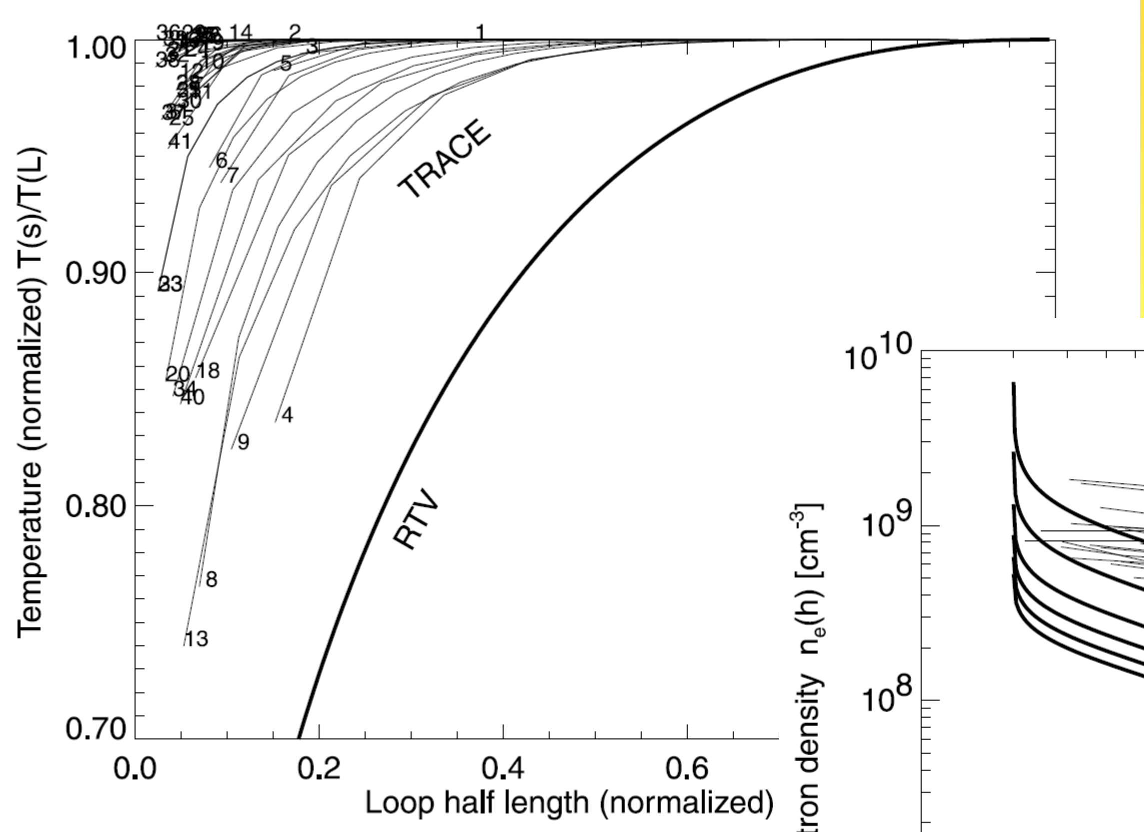

Aschwanden et al. (2000), ApJ 541, 1059

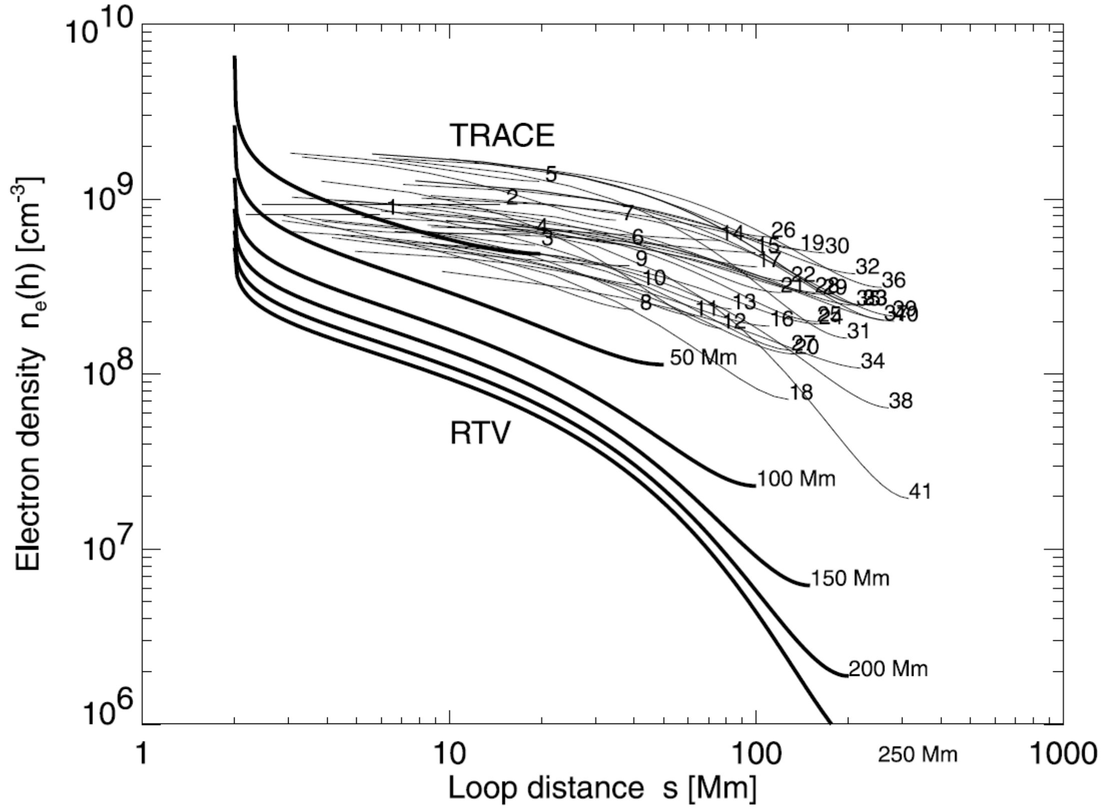

Proposed heating models

Lundquist et al. 2008, ApJ 689, 1388

TABLE 1
HEATING SCALE RELATIONSHIPS

Description	Number	Reference	MDK Scaling	B Case a	B Case b	B Case c	L
Stochastic buildup	1	1	$B^2L^{-2}V^2\tau$	B^2	B^1	B^2	L^{-2}
Critical angle	2	2	$B^2L^{-1}V^1\tan\theta$	B^2	$B^{1.5}$	B^2	L^{-1}
Critical twist	3	3	$B^2L^{-2}V^1R^1\phi$	B^2	B^1	...	L^{-2}
Reconnection $\propto v_A$	4	4	$B^1L^{-2}\rho^{0.5}V^2R^1$	B^1	...	$B^{0.5}$	$L^{-2.45}$
Reconnection $\propto v_{A\perp}$	5	5	$B^{1.5}L^{-1.5}\rho^{0.25}V^{1.5}R^{1.5}$	$B^{1.5}$	...	$B^{0.75}$	$L^{-1.725}$
Current layers (DC)	6	6	$B^2L^{-2}V^2\tau\log R_m$	B^2	...	...	L^{-2}
	7	7	$B^2L^{-2}V^2S^{0.1}\tau$	B^2	...	...	L^{-2}
	8	8	$B^2L^{-2}V^2\tau$	B^2	...	...	L^{-2}
Current sheets	9	9	$B^2L^{-1}R^{-1}V_{ph}^2\tau$	B^2	...	$B^{2.5}$	L^{-1}
Taylor relaxation	10	10	$B^2L^{-2}V_{ph}^2\tau$	B^2	...	...	L^{-2}
Turbulence (DC) with:							
Constant dissipation coefficients	11	11	$B^{1.5}L^{-1.5}\rho^{0.25}V^{1.5}R^{1.5}$	$B^{1.5}$	...	$B^{0.75}$	$L^{-1.725}$
Closure	12	12	$B^{1.67}L^{-1.33}\rho^{0.17}V^{1.33}R^{0.33}$	$B^{1.67}$	...	$B^{1.505}$	$L^{-1.483}$
Closure + spectrum ($s = 0.7$)	13	13	$B^{1.7}L^{-1.7}\rho^{0.15}V^{1.3}R^{0.7}$	$B^{1.7}$	...	$B^{1.35}$	$L^{-1.835}$
Closure + spectrum ($s = 1.1$)	14	13	$B^{2.1}L^{-2.1}\rho^{-0.05}V^{0.9}R^{1.1}$	$B^{2.1}$	...	$B^{1.55}$	$L^{-2.055}$
Resonance ($m = -1$)	15	14	B^0L^{-2}	B^0	...	...	L^{-2}
Resonance ($m = -2$)	16	14	$B^{-1}L^{-1}\rho^{0.5}$	B^{-1}	...	...	$L^{-1.45}$
Resonant absorption I ($m = -1$)	17	15	B^0L^0	B^0	...	...	L^0
Resonant absorption I ($m = -2$)	18	15	$B^{-1}L^1\rho^{0.5}$	B^{-1}	...	...	$L^{0.55}$
Resonant absorption II ($m = -1$)	19	16	$B^0L^1\rho^1$	B^0	...	...	$L^{0.1}$
Resonant absorption II ($m = -2$)	20	16	$B^{-1}L^2\rho^{1.5}$	B^{-1}	...	...	$L^{0.65}$
Current layers (AC)	21	17	$B^1L^{-1}\rho^{0.5}V^2$	B^1	...	...	$L^{-1.45}$
Turbulence (AC)	22	18	$B^{1.67}L^{-1.33}R^{0.33}$	$B^{1.67}$	...	$B^{1.505}$	$L^{-1.33}$

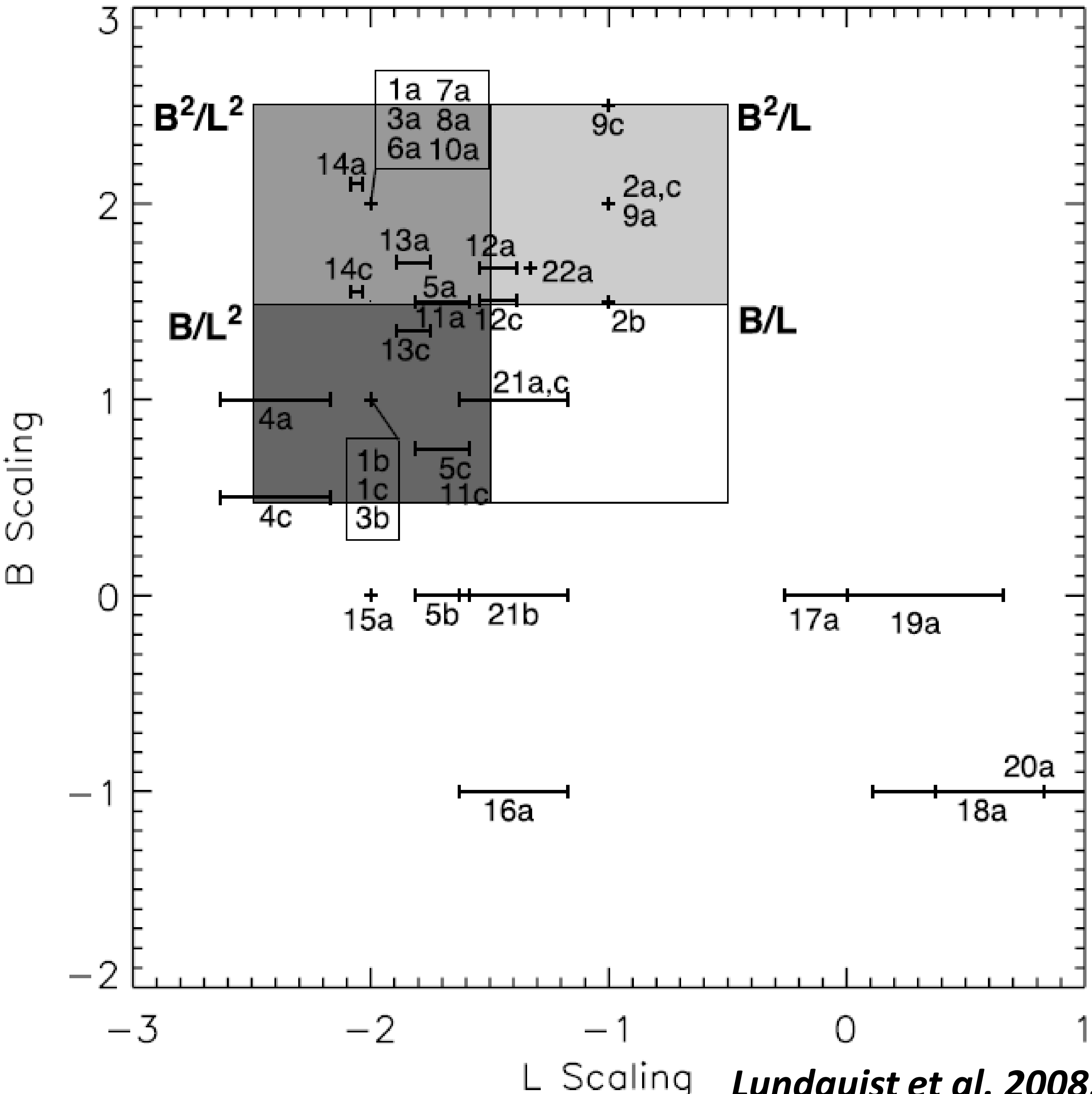

Lundquist et al. 2008, ApJ 689, 1388

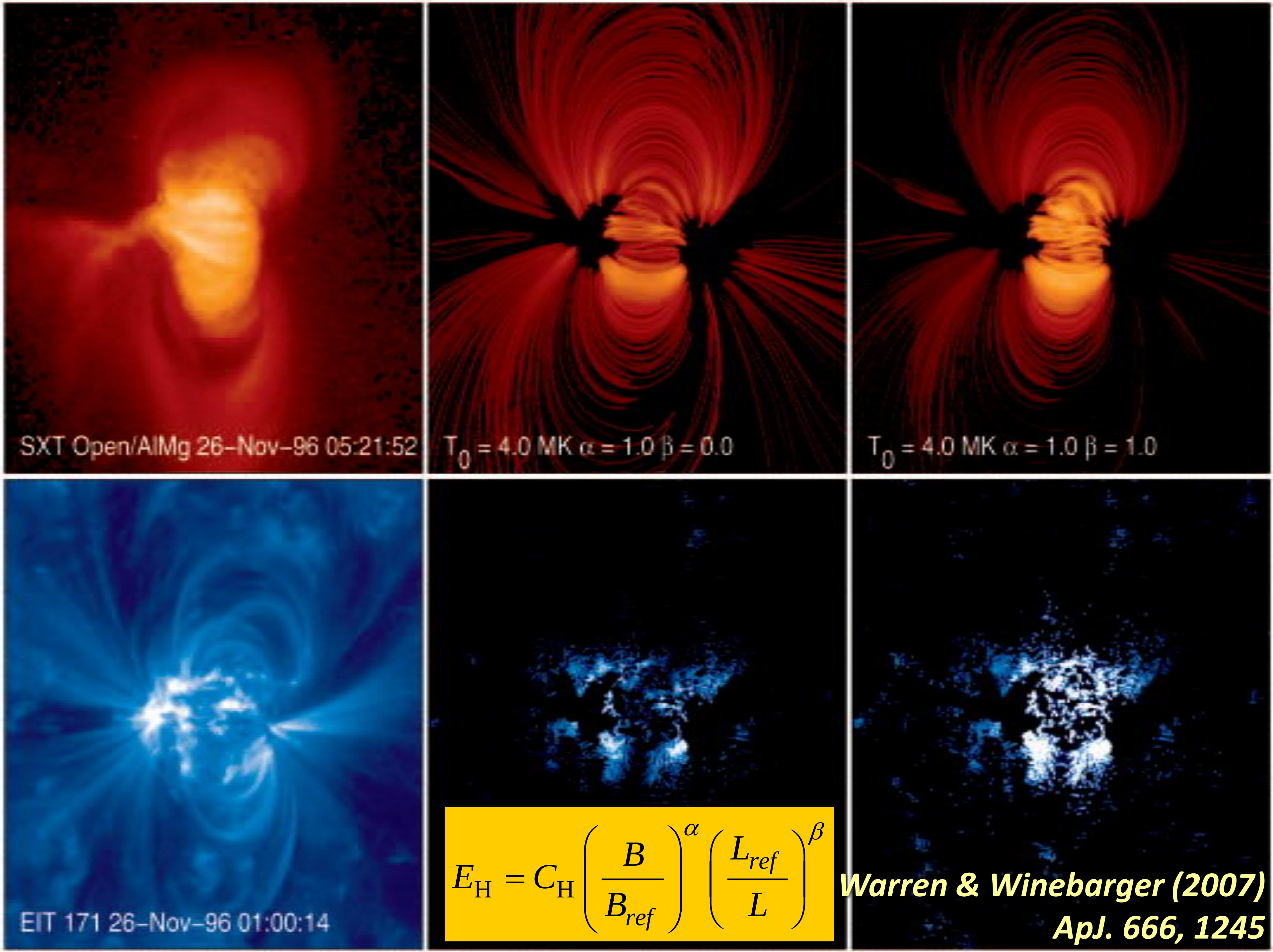

$$E_{\mathrm{H}} = C_{\mathrm{H}} \left(\frac{B}{B_{ref}} \right)^{\alpha} \left(\frac{L_{ref}}{L} \right)^{\beta}$$

Warren & Winebarger (2007)
ApJ. 666, 1245

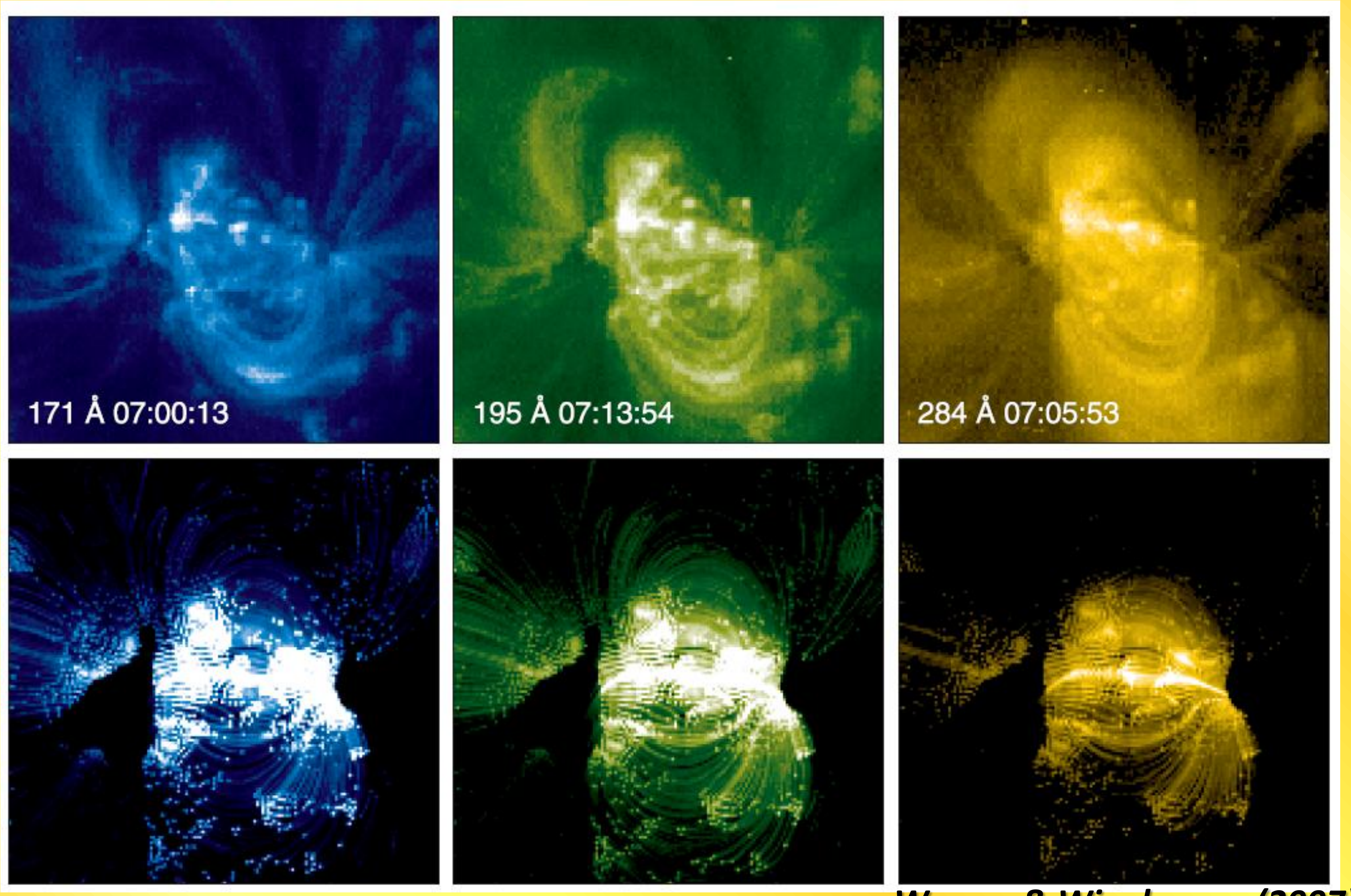

Warren & Winebarger (2007)
ApJ. 666, 1245

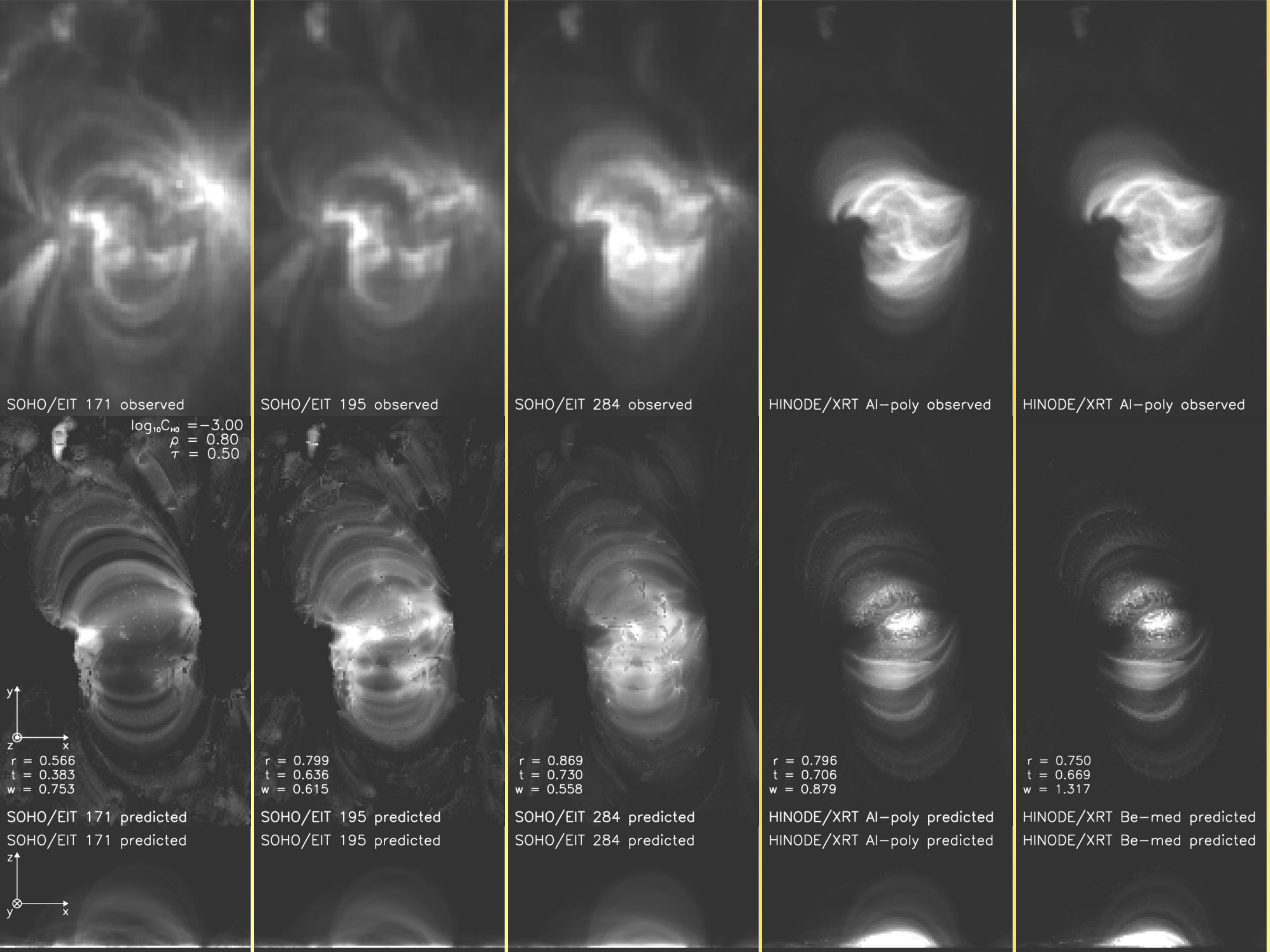
SOHO/EIT 171 observed
SOHO/EIT 195 observed
SOHO/EIT 284 observed
HINODE/XRT Al–poly observed
HINODE/XRT Al–poly observed
log₁₀C_H0 =–3.00
ρ = 0.80
τ = 0.50
y
z
x
r = 0.566
t = 0.383
w = 0.753
SOHO/EIT 171 predicted
r = 0.799
t = 0.636
w = 0.615
SOHO/EIT 195 predicted
r = 0.869
t = 0.730
w = 0.558
SOHO/EIT 284 predicted
r = 0.796
t = 0.706
w = 0.879
HINODE/XRT Al–poly predicted
r = 0.750
t = 0.669
w = 1.317
HINODE/XRT Be–med predicted
SOHO/EIT 171 predicted
SOHO/EIT 195 predicted
SOHO/EIT 284 predicted
HINODE/XRT Al–poly predicted
HINODE/XRT Be–med predicted
z
y
x

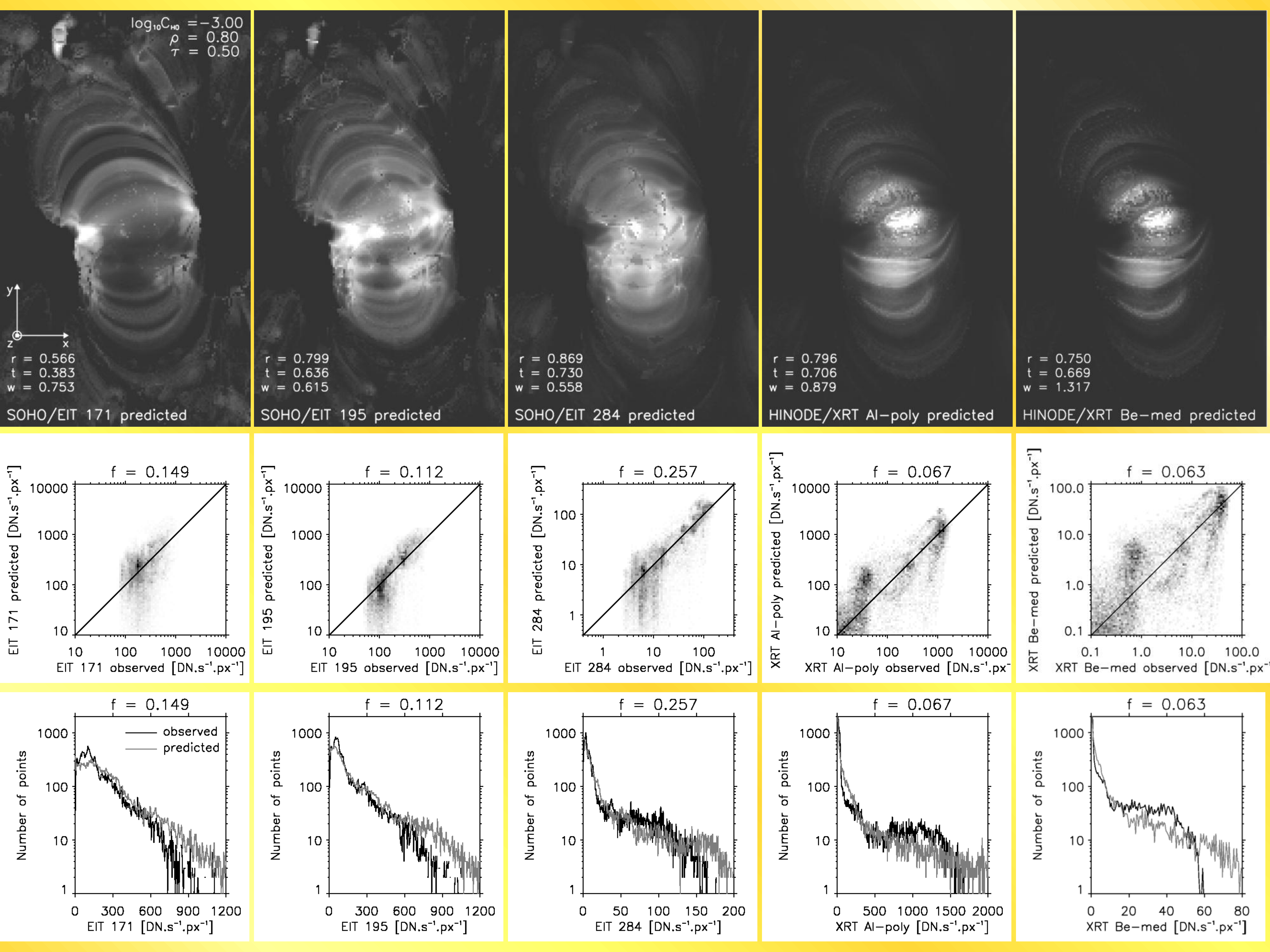

log10CH0 = −3.00
ρ = 0.80
τ = 0.50
r = 0.566
t = 0.383
w = 0.753
SOHO/EIT 171 predicted
r = 0.799
t = 0.636
w = 0.615
SOHO/EIT 195 predicted
r = 0.869
t = 0.730
w = 0.558
SOHO/EIT 284 predicted
r = 0.796
t = 0.706
w = 0.879
HINODE/XRT Al−poly predicted
r = 0.750
t = 0.669
w = 1.317
HINODE/XRT Be−med predicted
f = 0.149
EIT 171 predicted [DN.s⁻¹.px⁻¹]
EIT 171 observed [DN.s⁻¹.px⁻¹]
f = 0.112
EIT 195 predicted [DN.s⁻¹.px⁻¹]
EIT 195 observed [DN.s⁻¹.px⁻¹]
f = 0.257
EIT 284 predicted [DN.s⁻¹.px⁻¹]
EIT 284 observed [DN.s⁻¹.px⁻¹]
f = 0.067
XRT Al−poly predicted [DN.s⁻¹.px⁻¹]
XRT Al−poly observed [DN.s⁻¹.px⁻¹]
f = 0.063
XRT Be−med predicted [DN.s⁻¹.px⁻¹]
XRT Be−med observed [DN.s⁻¹.px⁻¹]
observed
predicted
Number of points
EIT 171 [DN.s⁻¹.px⁻¹]
EIT 195 [DN.s⁻¹.px⁻¹]
EIT 284 [DN.s⁻¹.px⁻¹]
XRT Al−poly [DN.s⁻¹.px⁻¹]
XRT Be−med [DN.s⁻¹.px⁻¹]

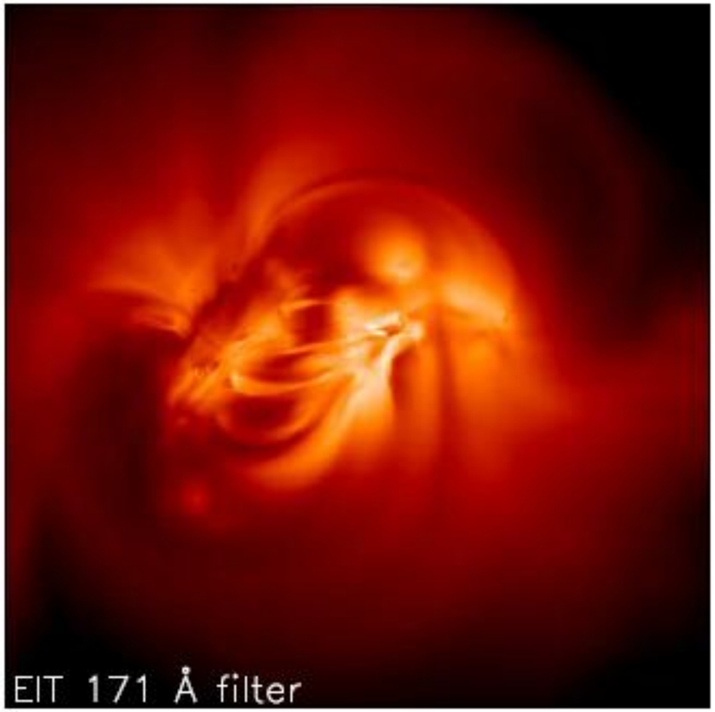

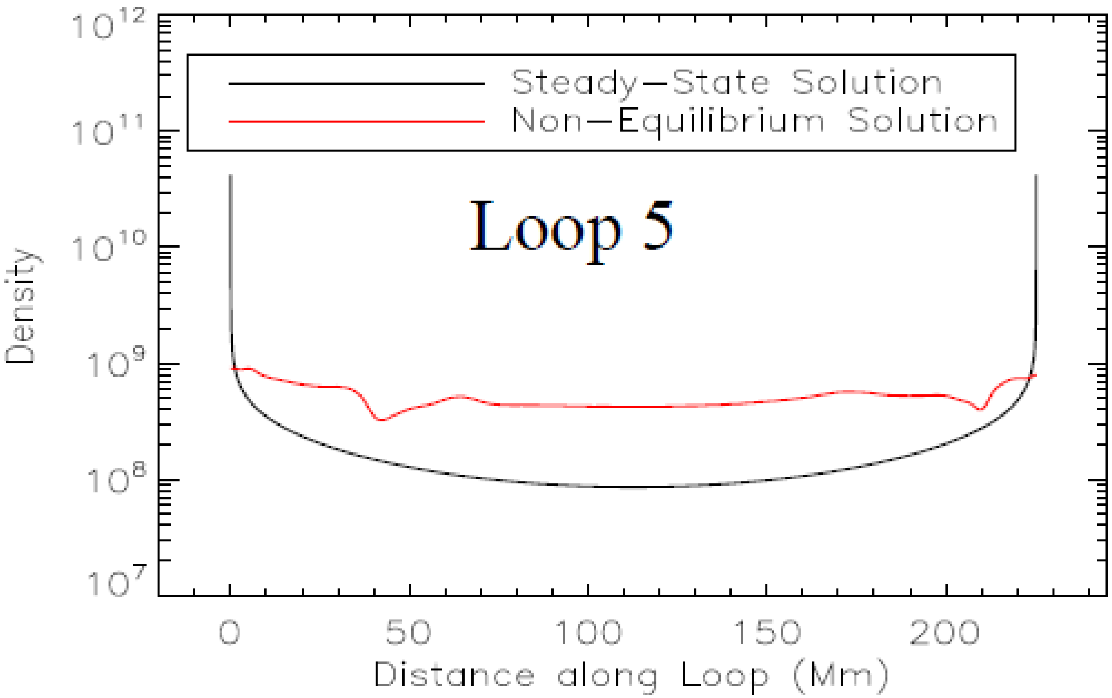

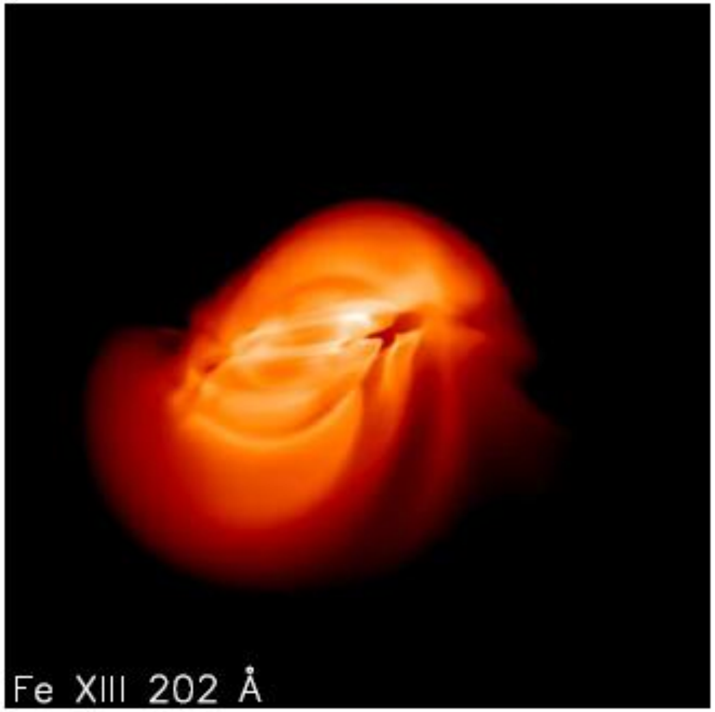

Lionello et al. (2011)
Loops Workshop V presentation

Thermal nonequilibrium

1. If the heating is too localized near the footpoints, the thermal conduction cannot balance the radiative losses near the apex.
2. As a result, loop apex cools.
3. Cooling increases radiative losses!
4. Condensation develops, grows and falls down. Loop empties.
5. Empty loop is heated, resulting in chromospheric evaporation. **Cycle renews.**

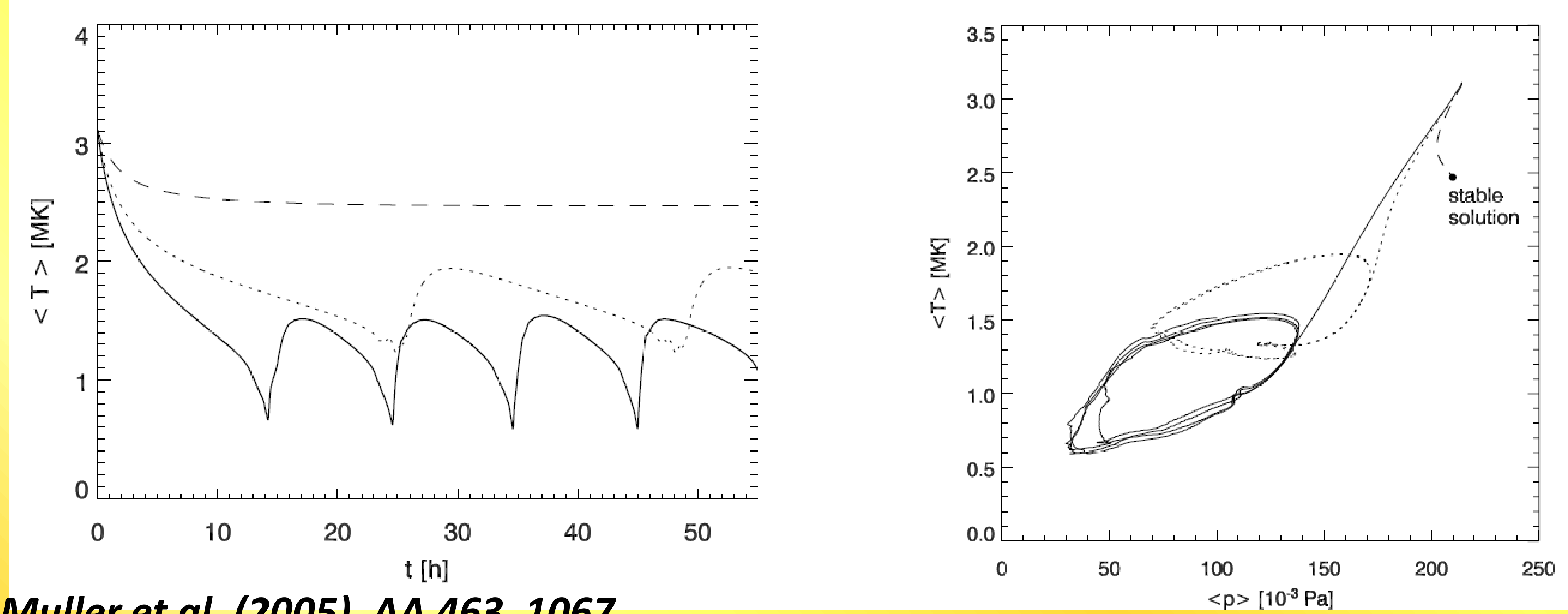

Muller et al. (2005), AA 463, 1067

Nanoflare storms

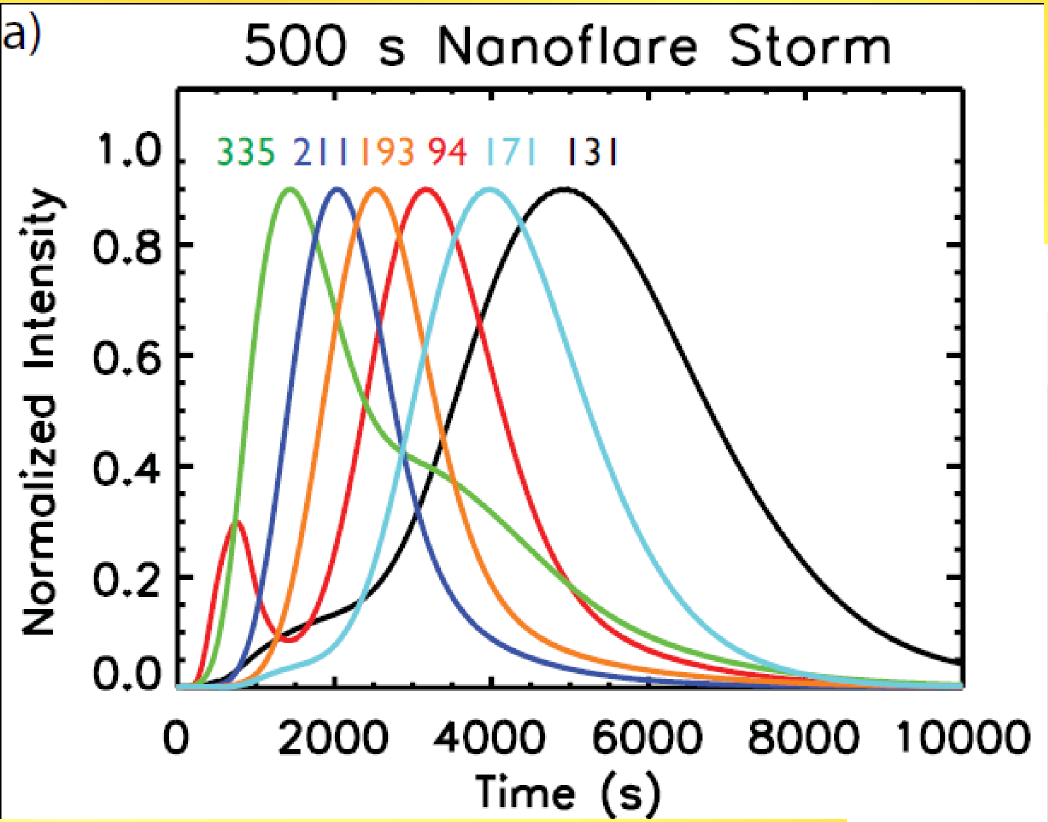

- Multi-strand loop
- One strand heated at a time, then next one is heated

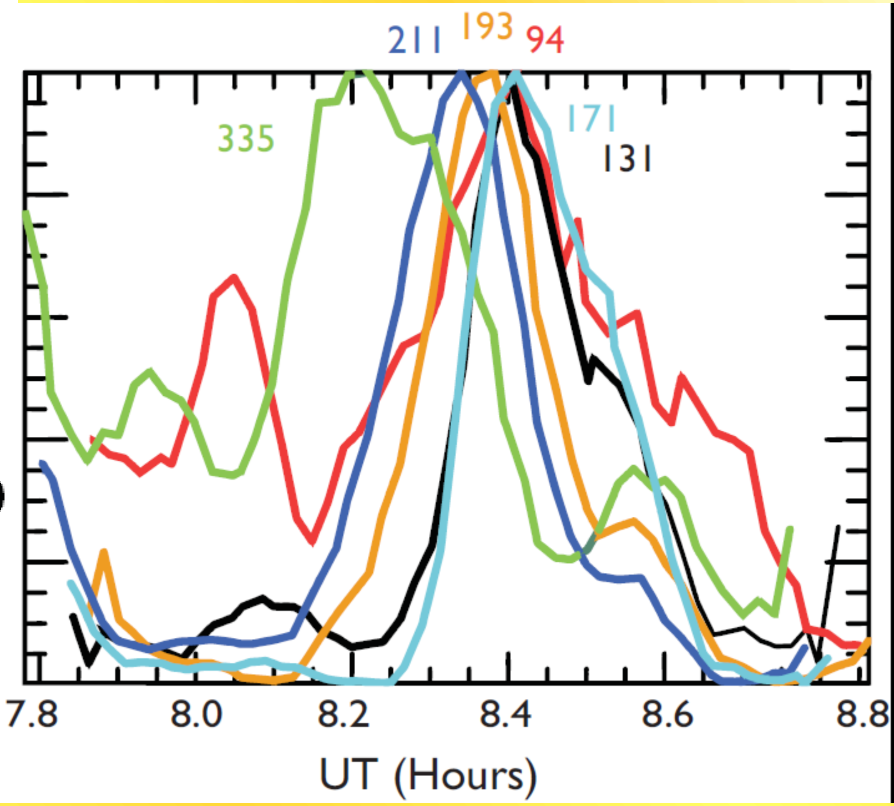

Theoretical light curves ^

Observed light curves >
for an AR core loop

Viall & Klimchuk (2011), ApJ 738, 24

Concluding remarks

- The solar corona is a rather fascinating environment
- Corona is NOT well understood, especially the heating part
- But significant progress in the last 3-4 decades
- For now, imaging spectroscopy is the way to go: push for high spatial, temporal, AND spectral resolution at the same time
- Theoretical modeling becomes routine.

Thank you for your attention!

(I hope you learned something)